

© 2021

HUAN HUANG

ALL RIGHTS RESERVED

OPTIMIZING DEPOSITION OF MATRIX AND IONIZATION SALT VIA TWO-STEP  
SUBLIMATION IN SAMPLE PREPARATION FOR SURFACE-LAYER MATRIX-  
ASSISTED LASER DESORPTION/IONIZATION TIME-OF-FLIGHT MASS  
SPECTROMETRY IMAGING (SL-MALDI-TOF MSI)

A Thesis

Presented to

The Graduate Faculty of the University of Akron

In Partial Fulfillment

of the Requirements for the Degree

Master of Science

Huan Huang

May, 2021

OPTIMIZING DEPOSITION OF MATRIX AND IONIZATION SALT VIA TWO-STEP  
SUBLIMATION IN SAMPLE PREPARATION FOR SURFACE-LAYER MATRIX-  
ASSISTED LASER DESORPTION/IONIZATION TIME-OF-FLIGHT MASS  
SPECTROMETRY IMAGING (SL-MALDI-TOF MSI)

Huan Huang

Thesis

Approved:

Accepted:

---

Advisor  
Dr. Mark D. Foster

---

Interim Director of SPSPE  
Dr. Ali Dhinojwala

---

Committee Member  
Dr. Chrys Wesdemiotis

---

Interim Dean of the College  
Dr. Craig Menzemer

---

Interim Director, Graduate School  
Dr. Marnie Saunders

---

Date

## ABSTRACT

Studying the surface behavior of polymers is crucial to improve many applications of polymers or enlarge the range of applications. Surface Layer Matrix-Assisted Laser Desorption/Ionization Time-of-Flight Mass Spectrometry Imaging (SL-MALDI-TOF MSI) is a novel technique based on the widely applied method of conventional MALDI mass spectrometry. Through SL-MALDI-TOF MSI, visualization of surfaces can be achieved. Moreover, this surface-specific technique can obtain the molecular composition of the surface layer, which we define as the layer within a few nanometers of the surface. Also, one can image the variation in this composition laterally across the surface. Previous research has proven that a two-step sublimation process of matrix and ionization salt is the best sample preparation for SL-MALDI MSI analysis. Nevertheless, the reproducibility and fidelity of the MALDI imaging still remain unsatisfying.

From the preliminary investigations on the factors leading to nonuniform SL-MALDI-MSI signals from uniform film samples, it was concluded that the distributions of matrix and ionization salt in the chamber during sublimation are only two of the possible factors impacting uniformity, while thermal gradients

were suspected to be a main factor causing the low fidelity. After eliminating thermal gradients from various aspects of the deposition process, the probability of obtaining a SL-MALDI image with high fidelity is greatly increased. However, the technique still suffers from low reproducibility and the occasional appearance of a secondary distribution in the mass spectra resulting from the salt clusters. A speculation is made suggesting that these limitations can be overcome potentially by using proper pretreatment for the ionization salt.

## ACKNOWLEDGEMENTS

I would like to thank my advisor, Dr. Mark D. Foster, for his help in the project and also his guidance and suggestions.

I would like to thank Dr. Wesdemiotis, for his assistance and allowing access to his equipment.

I would like to thank Kayla Williams-Pavlantos and Brenna Rossi for their helpful discussions about this project and their help in carrying out the experiments.

Thanks to my group members, my friends, and my parents.

Thanks to the University of Akron.

## TABLE OF CONTENTS

LIST OF FIGURES .....	ix
LIST OF TABLES.....	xiii
CHAPTER	
I. INTRODUCTION.....	1
II. BACKGROUND.....	4
2.1 Surface behavior of polymers and characterization methods .....	4
2.1.1 Surface behaviors of polymers.....	4
2.1.2 Characterization and challenges.....	5
2.2 MALDI-TOF MS .....	7
2.3 Surface Layer MALDI-TOF MSI.....	12
2.4 Sample preparation for SL-MALDI-TOF MSI .....	16
2.4.1 Deposition methods for matrix and ionization salt.....	16
2.4.2 Two-step sublimation .....	18
III. EXPERIMENTAL .....	21
3.1 Materials .....	21
3.2 Preparation of PS thin films .....	23
3.3 Two-step sublimation .....	24
3.4 Characterization of samples .....	26

IV. RESULTS AND DISCUSSION .....	29
4.1 Nonuniformity of the deposited layer .....	29
4.2 Possible factors causing the nonuniform deposition.....	34
4.3 Investigation on distributions of matrix and salt.....	37
4.3.1 Matrix distribution.....	38
4.3.2 Salt distribution .....	41
4.4 Elimination of thermal gradients .....	43
4.4.1 Efforts in eliminating thermal gradients .....	44
4.4.2 Results of eliminating thermal gradients .....	46
4.5 Optimization of sublimation conditions .....	49
4.5.1 Matrix/salt amount and sublimation time .....	49
4.5.2 Elimination of salt clusters.....	52
4.5.3 Necessity of salt pretreatment.....	54
V. CONCLUSION .....	59
REFERENCES .....	63



## LIST OF FIGURES

Figure	Page
2.1: Illustration of the desorption/ionization process in MALDI. The arrow with black outline represents the direction that ions move under the influence of an external electric field.....	9
2.2: Schematic of a linear TOF instrument analyzing ions produced by MALDI. The figure is adapted from Hill's thesis.....	10
2.3: Schematic of a reflection-mode TOF instrument analyzing ions produced by MALDI. The figure is adapted from Hill's thesis.....	10
2.4: Illustration of the desorption/ionization process in surface-layer MALDI. Matrix and ionization salt are deposited onto the sample surface. Hence only analyte molecules sitting at the sample surface are desorbed and ionized. The arrow with black outline represents the direction that ions move under the influence of an external electric field.....	13
3.1: Conventional bulk spectrum of the 6 kDa PS. The spectrum has a distribution from m/z of about 4000 to about 7700. The distribution indicates a repeat unit molecular mass of 104.4 Da.....	22
3.2: Schematic of sublimation apparatus.....	24
4.1: Tapping mode height sensor image of 6K PS film. The gradient of the color scale bar represents the height variation across the scanned region on the sample surface. The root mean square roughness obtained from this image is $R_q = 0.489$ nm.....	30
4.2: False color SL-MALDI images of three 6K PS thin film samples. For each sample, three long rectangular regions have been scanned. The gradient of color on the scale to the right of the image represents a linear variation	

	in signal intensity and is based on spectra intensity relative to the highest intensity for the entire sample.....	30
4.3:	(a), (b) and (c) are tapping mode AFM height images from three different spots on one sample after two-step sublimation. (d), (e) and (f) are corresponding tapping mode AFM phase images collected simultaneously with (a), (b) and (c).....	32
4.4:	(a) Schematic showing the bottom up view of the cold finger bottom with two 2 cm × 2 cm samples attached to the edge. The gradient of the false color scale bar represents the vertical distance from the outer wall of the cold finger to the reverse face of the samples. (b) Schematic showing a cross section view of the lower parts of the cold finger and the chamber.....	35
4.5:	The distribution of 50 mg DCTB (left) and 50 mg AgTFA (right) at the bottom inside of the chamber creating by the regular operation.....	36
4.6:	Schematic showing the distributions of matrix and salt for different samples. (a) Distributions for Samples 2 and 3, for which the matrix travels a much shorter path length to get to the surface of Sample 3 than to the surface of Sample 2, while the salt travels for a similar path length to get to the surfaces of the two samples. (b) Distributions for Samples 4 and 5, for which the salt travels a much shorter path length to get to the surface of Sample 4 than to the surface of Sample 5, while the salt travels for a similar path length to get to the surfaces of the two samples.....	38
4.7:	(a) SL-MALDI image of sample 1 which was prepared by two-step sublimation with regular distributions of both matrix and ionization salt. (b) Spectrum of one pixel with the highest intensity selected from the SL-MALDI image in (a).....	39
4.8:	(a) and (b) are the SL-MALDI images of two samples prepared simultaneously with regular distribution of ionization salt, but with different distributions of matrix. Sample 3 with matrix right beneath it gave the	

	image in (b), while Sample 2 attached on the opposite edge of the cold finger gave the image in (a). (c) and (d) are the spectra of one pixel with the highest intensity selected from the SL-MALDI images in (a) and (b), respectively.....	40
4.9:	(a) and (b) are the SL-MALDI images of two samples prepared simultaneously with regular distribution of matrix, but with different distributions of ionization salt. The sample with salt right beneath it gave the image in (b), while the sample attached on the opposite edge of the cold finger gave the image in (a). (c) and (d) are spectra of one pixel with the highest intensity selected from the SL-MALDI images in (a) and (b), respectively.....	42
4.10:	(a) Schematic showing the view looking up at the modified cold finger bottom with one 2 cm × 2 cm sample attached to the middle. The gradient of the false color scale bar represents the vertical distance from the outer wall of the cold finger to the back face of the sample. (b) Schematic showing the vertical cross section view of the lower parts of the modified cold finger and the rebuilt chamber.....	45
4.11:	A matrix layer prepared from 50 mg of DCTB using the solvent evaporation method.....	46
4.12:	SL-MALDI images of two of the good samples obtained after all efforts of eliminating the thermal gradients were done.....	47
4.13:	Mass spectrum corresponding to one pixel from the SL-MALDI image measured for one of the samples. The primary distribution is the mass distribution of 6K PS, with a spacing of ~104 Da. The secondary distribution shown in the blue box corresponds to the mass distribution of the silver salt clusters.....	48
4.14:	SL-MALDI images of samples from group S1 (a), S2 (b), S3 (c), S4 (d), S5 (e) and S6 (f).....	50

4.15: SL-MALDI images of three samples prepared using the conditions in group S2. The signal intensities are much less uniform than those in Figure 4.14(b).....	51
4.16: (a) 10 $\mu\text{m}$ $\times$ 10 $\mu\text{m}$ height sensor image measured by tapping mode AFM from a sample with only matrix deposited on the surface. The root mean square roughness obtained from this region is $R_q = 148$ nm. (b) 10 $\mu\text{m}$ $\times$ 10 $\mu\text{m}$ height sensor image measured by tapping mode AFM from a sample after salt deposition with a $R_q = 272$ nm. (c) The height variations along the section lines in (a) and (b).....	56
4.17: (a) and (b) are the photographs showing the distributions of 40 mg of two AgTFA salt products in chamber. (c) and (d) are the zoom-in views of the middle parts in (a) and (b), respectively.....	58

## LIST OF TABLES

Table	Page
3.1: Optimized conditions for two-step sublimation.....	24
4.1: Distribution of matrix and salt investigated.....	37
4.2: Sublimation conditions investigated for S1-S6.....	49
4.3: Conditions of salt sublimation and results for samples C1-C5.....	53

## CHAPTER I

### INTRODUCTION

The surface sits between a material and the surrounding environment. The character of the surface dictates many important properties of a material, such as adhesiveness, corrosion resistance and absorption. It is of both fundamental and practical importance to understand the composition and morphology at the surface.

Characterization techniques used to detect features of the surface at the molecular level should have high sensitivity because only a small amount of sample will be probed if the characterization is truly restricted to the material right at the surface. Moreover, it is crucial that the signal level remains high across the whole sample surface and varies faithfully with the local character of the surface. There are different kinds of surface-sensitive characterization techniques that have been applied in research on polymeric surfaces such as Time-of-flight secondary ion mass spectrometry (TOF SIMS), X-ray photoelectron spectroscopy (XPS), X-ray reflectivity (XR), and neutron reflectivity (NR). Among these techniques, Surface Layer Matrix-Assisted Laser Desorption/Ionization

Mass Spectrometry (SL-MALDI MS) has significant advantages not only as a label free method, which avoids artifacts due to labelling, but also as a technique that yields direct information about the entire polymer chains and about the distribution of various chains rather than just about fragments of the polymer chains.

Surface Layer Matrix-Assisted Laser Desorption/Ionization Mass Spectrometry Imaging, or SL-MALDI MSI is a technique based on SL-MALDI MS, that provides two dimensional images of the surface of polymer films. Recent efforts at further developing this technique have focused on theoretical analysis of polymer surface behavior, exploration of key factors for imaging quality, as well as optimization of the sample preparation process.<sup>1-2</sup> This technique has great potential to assist in understanding polymeric surface behavior and investigate complex situations.

To obtain an image with high intensity and good fidelity using SL-MALDI MSI, matrix and ionization agent need to be applied to the sample. Common methods to apply matrix onto samples are solvent based, which inevitably affect the sample surface. Sublimation, however, is a solvent-free method, causing little perturbation to the sample surface.

To apply SL-MALDI-TOF MSI to the characterization of synthetic polymers, it is important that the acquired images and data give consistent results. Nevertheless, a sample preparation method that guarantees reproducibility and fidelity has not been reported so far. The focus of this work has been to optimize the sample preparation process and conditions to provide reproducibility and fidelity, as well as improve signal intensity for this technique. Previous work has shown that sublimation of the matrix and ionization agent separately (i.e. two-step sublimation), gives better results than does sublimating the two simultaneously.<sup>3-4</sup> To further improve the quality of images acquired from SL-MALDI MSI analysis, the focus of this thesis is to determine the factors in two-step sublimation leading to low reproducibility, fidelity and intensity as well as to optimize the sublimation process.



## CHAPTER II

### BACKGROUND

#### 2.1 Surface behavior of polymers and characterization methods

##### 2.1.1 Surface behaviors of polymers

In polymeric systems, the molecular composition at the surface is usually different from that in the bulk, as the result of “surface segregation” of some species in the material, since in practical applications, blends of materials are very widely used. This segregation occurs over a depth of the order of the radius of gyration of the polymer molecules adjacent to the surface. In almost all polymer blends, one of the components will be preferred at the surface. Even for a polymer material that we normally think of as containing only one kind of molecule, surface segregation can still be observed due to the polydispersity of chain molecular weight of this one sort of polymer. Chains of each molecular weight constitute different components of a complex blend.

The state a polymer system adopts at equilibrium minimizes the overall free energy of that system by having the proper surface composition.<sup>5</sup> The free energy is determined by both entropic effects and enthalpic effects. In a single component system, where the only differences among polymer chains are among their molecular weights, entropic effects will drive the shorter chains to the surface. This is due to the fact that the number of configurations a chain can take at the surface is constrained by the strongly asymmetric environment for the chains at the surface and the fact that shorter chains will experience a smaller loss of configurations when driven from the bulk to the surface.<sup>6</sup>

### 2.1.2 Characterization and challenges

To properly determine the molecular composition across the surface of a polymer material, a characterization technique should meet several requirements. First of all, since the targeted region of the measurement is the surface layer, the probing depth of the technique should be of the order of a nanometer. In addition, to obtain the true and accurate information of the molecular composition, the measurement itself and the sample preparation process for the measurement should not cause alteration to the surface.

There are multiple surface-sensitive characterization techniques that can be used to determine the chemical composition at polymer surfaces, such as X-ray photoelectron spectroscopy (XPS), secondary ion mass spectrometry (SIMS), surface-enhanced Raman spectroscopy (SERS) and tip-enhanced Raman spectroscopy (TERS). XPS composition measurement can readily be made quantitative. However, XPS can only detect the elemental composition, and is not sensitive to hydrogen. For synthetic polymers that are hydrocarbon based, the focus then is on quantifying the presence of carbon and oxygen in polymers and variations in their bonding. Therefore, it can be difficult to differentiate two hydrocarbon polymer molecules in XPS analysis. During SIMS measurements, a focused primary beam is used to sputter the sample surface, which will cause significant fragmentation to the polymer molecules. Therefore, the technique is unable to determine the molecular weight of polymer chains. The quantification of the polymer fragments is also very difficult.

SERS and TERS are techniques based on Raman spectroscopy. Both are able to provide fingerprints of polymer molecules at the polymer surface in a non-destructive way. However, neither the quantification of the molecular composition nor the lateral resolution is available from SERS measurements. With the incorporation of a tip, the detected region of a TERS spectrum can be limited to a

sub-micron area under the tip, enabling the technique to obtain laterally resolved information laterally on sample surface. Nevertheless, it is still difficult to obtain quantitative information.

A solution to this problem with characterizing the molecular composition on polymer surfaces is to use the technique, SL-MALDI-TOF MS, developed by the Wesdemiotis and Foster research group.<sup>7-8</sup> This is a truly surface-specific technique, meaning that it can detect the surface layer with a depth of only 1 to 2 nm, and requires no labelling. Since MALDI is one of the soft ionization methods, polymer chains can be ionized without fragmentation, which enables the information from the intact polymer chains to be detected. Further, Endres and Hill, et al.<sup>1</sup> developed the imaging technique, SL-MALDI-TOF MSI, which enables visualization of the molecular distribution across polymer surfaces.

## 2.2 MALDI-TOF MS

Mass spectrometry is a powerful analytical technique that measures the mass-to-charge ratios ( $m/z$ ) of ions in the gas phase. There are three main components within a mass spectrometer: the ionizer, the analyzer and the mass detector. During the analysis, the analyte is first ionized and transferred into the

gas phase. Then the analyte ions travel through the analyzer and are separated by their mass-to-charge ratio. Lastly, the ions travel to the mass detector for detection and analysis.<sup>9</sup> This technique has been widely used in characterizing polymers for its ability to determine compositional heterogeneity, identify end groups, and characterize structures of specific oligomers.

MALDI is one of the soft ionization methods which allows molecules to be desorbed and ionized with no or negligible fragmentation and hence allows intact molecules to be detected. The principle of a MALDI process is shown in Figure 2.1. Briefly, the ions are produced when a laser beam irradiates the mixture of analyte, chromophoric matrix and ionization agent. The matrix used in this process absorbs energy from the laser beam and then transfers the energy to the analyte molecules, so that the analyte molecules can be desorbed and transistioned into gas molecules. Unlike biological tissues, for which ionization can be promoted by protonation, the addition of ionization salts is required for many synthetic polymers.<sup>1, 10-11</sup>

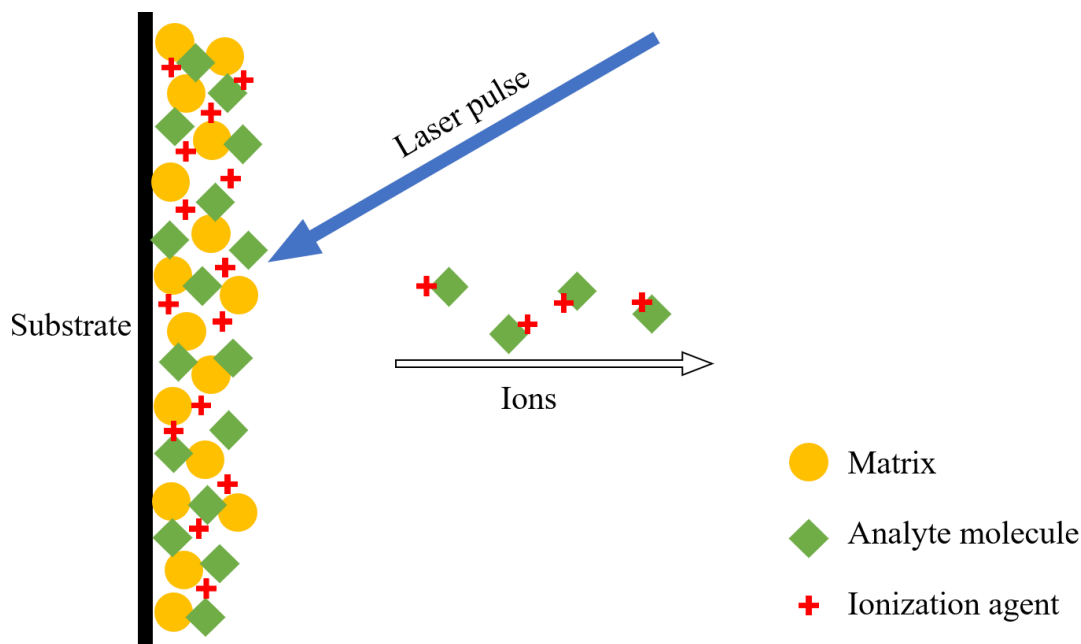


Figure 2.1: Illustration of the desorption/ionization process in MALDI. The arrow with black outline represents the direction that ions move under the influence of an external electric field.

MALDI is commonly combined with a time-of-flight (TOF) mass analyzer. The ions generated in the MALDI process are separated when travelling from one end of the TOF mass analyzer to the other end under an external electric field. The flight time an ion undergoes varies with the mass-to-charge ratio of the polymer ions. There are two different modes of TOF mass analyzers, linear and reflection modes, as shown in Figures 2.2 and 2.3, respectively. As the simpler mode, linear mode has been widely applied in polymer analysis.<sup>12</sup> In the reflection mode, the faster ions penetrate deeper into the reflectron than do other ions of same mass.

As a result, ions with the same mass, but different initial kinetic energies, arrive at the detector simultaneously. Therefore, a greater resolution can be achieved in the reflection mode. However, the signal intensity of the reflection mode is generally lower because there is a greater loss of ions when the ions are required to travel for a longer distance.

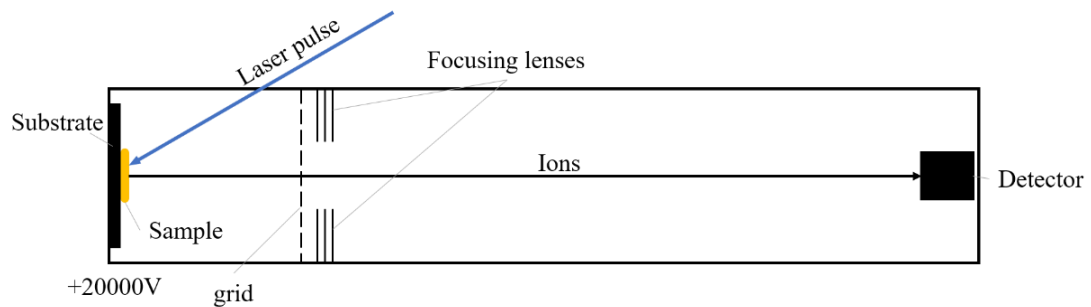


Figure 2.2: Schematic of a linear TOF instrument analyzing ions produced by MALDI. The figure is adapted from Hill's thesis.<sup>2</sup>

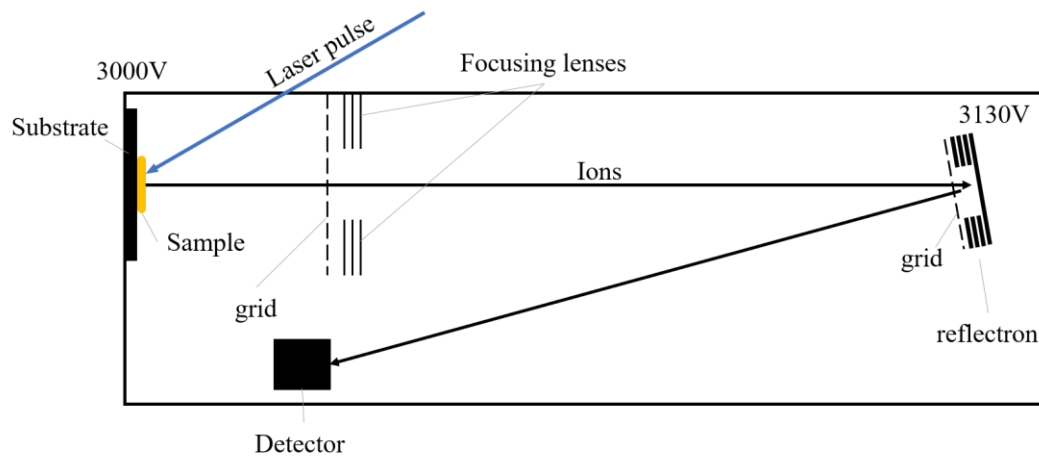


Figure 2.3: Schematic of a reflection-mode TOF instrument analyzing ions produced by MALDI. The figure is adapted from Hill's thesis.<sup>2</sup>

In comparison with other characterization techniques that can be used to determine the molecular weight of polymer samples, such as size-exclusion chromatography (SEC), vapor pressure osmometry (VPO), and light scattering (LS), MALDI-TOF MS can provide much more structural information in addition to the molecular weight distribution. Moreover, the interpretation of mass spectra obtained from MALDI-TOF MS measurements is relatively simple. The mass-to-charge ratios of the peaks in the spectrum directly correspond to the mass of the n-mer because the polymer ions are singly charged.

However, there are still a few limitations with MALDI-TOF MS analysis of synthetic polymers, among which the most common one is the low signal intensity from high molecular-weight polymers. Molecules with higher molecular weight are generally more difficult to desorb and ionize. The upper limit of molecular weight detectable for a synthetic polymer is much lower than that for a biopolymer.<sup>13</sup> An optimal matrix that has good miscibility with the polymer in the solid state and the addition of the proper cationization agent are crucial for successful characterization of synthetic polymers. What's more, polymer ions with larger mass will move slower in the TOF mass analyzer. This will lead to weaker signal intensity for larger polymer chains and therefore cause a distortion in the molecular weight distribution when the polymer has a wide polydispersity.



## 2.3 Surface Layer MALDI-TOF MSI

The most important feature of SL-MALDI-TOF MS is that only the surface layer at the surface of polymer sample is detected by the characterization, which is realized by depositing matrix and ionization salt only at the sample surface (Figure 2.4), rather than mixing the polymer together with matrix and ionization salt. It is necessary for polymers to contact the matrix directly in order to be desorbed. Therefore, with matrix condensed only at the sample surface, all polymer ions generated during the measurement should have originated from the surface layer within a specific thickness. Wang et al.<sup>7-8</sup> reported the thickness of the detected surface layer, which is also the depth resolution of this newly developed technique, to be smaller than 2 nm.

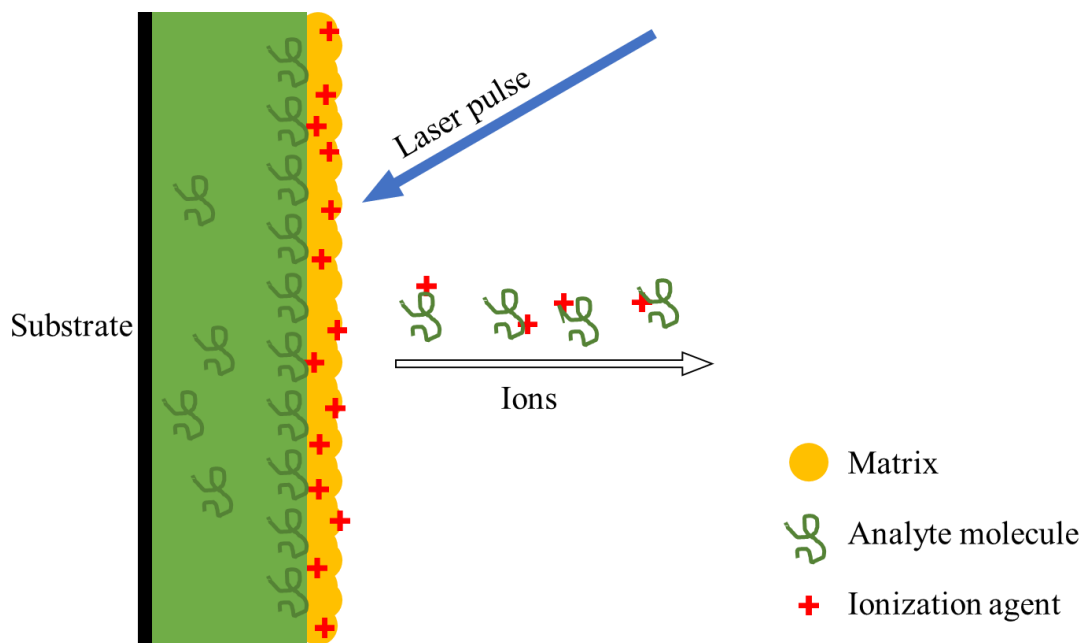


Figure 2.4: Illustration of the desorption/ionization process in surface-layer MALDI. Matrix and ionization salt are deposited onto the sample surface. Hence only analyte molecules sitting at the sample surface are desorbed and ionized. The arrow with black outline represents the direction that ions move under the influence of an external electric field.

In the research of Wang et al.,<sup>7-8</sup> SL-MALDI-TOF MS was used to determine the composition of a blend of cyclic and linear chains and the experimental results were compared with the prediction of self-consistent field (SCF) theory. No solvent was used for the purpose of avoiding perturbation to the sample surface. Instead, the matrix and ionization salt were ground up together and then directly spread on the polymer blend film. The results proved that this technique is truly surface-specific. By performing measurement on a bilayer film with a Langmuir monolayer of poly (methyl methacrylate) (PMMA) deposited on top of a spun cast 4 kDa

polystyrene (PS) film, the probing depth of the technique was confirmed to be 1 to 2 nm because only signals from the PMMA monolayer were detected. This probing depth is approximately equal to the radius of gyration of the 4 kDa PS.

Using a combination of TOF SIMS and SL-MALDI-TOF MS, Fouquet et al.<sup>14</sup> obtained a depth profile of a polymer bilayer composed of two PS layers with different molecular weights. Since the only difference between the molecules in the two layers was the molecular weight, SIMS was not able to differentiate the molecules from the two layers. In contrast, it was shown that SL-MALDI-TOF MS measurement was capable of obtaining the accurate distribution of molecular weight. By alternating SL-MALDI-TOF MS measurements with sputtering of the sample using the SIMS technique, a depth profile of the molecular composition was obtained, which clearly showed the composition gradient from the top layer to the bottom layer.

Hill et al.<sup>15</sup> applied SL-MALDI-TOF MS to study the surface segregation behavior of polymer systems. In thin film samples made from either anionically polymerized PS or anionically polymerized PMMA, short chains were found to enrich the surfaces due to entropic effects. Such anionically polymerized materials are routinely viewed as being monodisperse and it has been long assumed that the concentration of a specific n-mer at the surface is the same as that in the bulk.

Enthalpic effects driving surface segregation behavior were also investigated using this technique.<sup>16</sup> It was shown that at the surface of a blend of 6 kDa PS and 6 kDa PS functionalized with hydroxymethyl ends, not only the end groups with high energy, but also all segments connected to the functionalized ends, were depleted from the surface,

Building on the earlier studies pursued in collaboration with Hill, Endres et al.<sup>1, 17</sup> applied sublimation, a solvent-free method to deposit matrix and ionization salt onto the sample surfaces. Before conducting SL-MALDI-TOF MSI, the sample surfaces were stamped, masked, scratched, or solvated, intentionally creating defects, which were later imaged successfully by the technique. The signal intensities within the imaged region could be showed in images using a false color scale. Therefore, the imaging enables visualization of the concentration of a specific kind of molecule across the sample surface because the concentration directly corresponds to signal intensity.

## 2.4 Sample preparation for SL-MALDI-TOF MSI

### 2.4.1 Deposition methods for matrix and ionization salt

The deposition of matrix and ionization salt is the most important part of the sample preparation process. There are different deposition methods that have been widely used in MALDI MS experiments, such as the “dried droplet” method and spraying. These methods are mostly solvent based. When the “dried droplet” method is used, the polymer to be analyzed and the matrix are dissolved in one certain solvent, and the resulting solution is deposited onto the MALDI target plate. After the solvent is evaporated, the “dried droplet” left on the plate is the region for characterization. The spraying method only requires the matrix to be dissolved in a solvent. And the matrix solution is sprayed onto the surface of the polymer sample either manually or with an automated sprayer. The characterization can be conducted after the solvent evaporates.

These solvent-based methods to deposit matrix can cause some problems for the reproducibility of MALDI MS measurements. The topographies of samples prepared using the “dried droplet” method is not consistent, resulting in inconsistent results. Another problem is that the solubility of the polymer and the matrix may differ in the solvent, which will limit the homogeneity of the deposited

sample. The spraying method is not suitable for SL-MALDI MS measurement, either. Any solvent contacting the surface of the polymer sample can potentially cause changes in the molecular composition of the surface layer.

Other so-called “solvent-free” methods have been explored recently, including dry spray<sup>18</sup>, mechanical homogenization techniques and sublimation. However, rigorously speaking, the dry spray method are not truly solvent-free. Solvent is still used to dissolve the matrix and transport the matrix at least close to the sample surface. The difference between the dry spray method and conventional spraying is that the matrix solution is sprayed out from a heated needle, making the solvent evaporate much faster and depositing the matrix with less solvent remaining in the matrix when it first contacts the sample. Mechanical homogenization techniques such as the ball milling method<sup>19-20</sup> are truly solvent-free, but their basic principle is to make the analyte and matrix very fine powders that can be mixed homogeneously. Only sublimation is a feasible method for SL-MALDI MS as there is no perturbation from solvent or external mechanical force to the sample surface during preparation. In addition, fortuitously, the matrix are purified during the sublimation process, decreasing the possibility of sample surface being contaminated from impurities in the matrix.

#### 2.4.2 Two-step sublimation

Endres et al.<sup>1</sup> used the sublimation method to deposit matrix and ionization salt onto samples with intentionally created defects. Although the signal intensities were weak, the defects were clearly observed in the SL-MALDI images obtained from the measurement, indicating that the sublimation method is a suitable deposition method. In further work, the weak intensity was explained as resulting from a low concentration of salt in the layer deposited on the sample surface. When the matrix and ionization salt are sublimated and deposited at the same time and at the same temperature, there will be much more matrix condensed on sample surface because the sublimation temperature for matrix is usually much lower than that for the ionization salt.

If the depositions of the matrix and ionization salt can be done in separate sublimation steps, i.e. using a two-step sublimation method, the concentration of ionization salt deposited on the sample can potentially be increased. By depositing the ionization salt first, Lu<sup>3</sup> reported an enhanced signal intensity. However, it appeared that signals were detected from some very small regions on the sample surface, which were believed to be the gaps in the ionization salt layer. Since the matrix was deposited after salt sublimation, the matrix formed an additional layer

on top of the salt layer. Only at the gaps in the salt layer were there contacts between polymer and matrix, which are necessary for successful desorption of the polymer.

Guo<sup>4</sup> further optimized the two-step sublimation method by switching the sublimation order of matrix and ionization salt. By depositing the matrix first, signals were detected from the whole surface of the sample and the signal intensity was further improved. However, when imaging a single-component polymer sample with very smooth surface and uniform thickness, the uniformity of signal intensity, which corresponds to the fidelity of the technique, remained unsatisfactory. The reproducibility of the measurement also needs to be improved. For more reliable analysis, it will be better if the overall signal intensity can be further increased.

Although there are already commercial products for automated deposition of matrix and ionization salt via sublimation such as the iMLayer (Shimadzu, Kyoto, Japan) and HTX sublimator (HTX-Technologies, Chapel Hill, North Carolina, USA), the costs of these products are usually very high, which means they are more suited for high-throughput applications like diagnostic or clinical uses. For researchers who have the need for studying surface behavior of synthetic polymers using SL-MALDI MSI, it will be more affordable to use an apparatus



based on standard glass sublimators available from various vendors. Such glass sublimators are unlikely to be able to provide the same level of coating reproducibility due to the less rigorous control over the heating of the chemicals, vacuum, and cooling of the samples possible in a glass vessel. Sublimators made from metals such as stainless steel<sup>21</sup> can potentially offer a more controlled process, but building a metal sublimator still requires much effort. In the thesis work presented here, we aim at providing a solution based on a standard glass sublimator by modifying the sublimation setup and optimizing the two-step sublimation method.

## CHAPTER III

### EXPERIMENTAL

#### 3.1 Materials

6 kDa linear PS was synthesized via anionic polymerization by a previous member of the Foster research group<sup>22</sup>. The molecular characteristics of this material were measured using conventional MALDI-TOF-MS (Figure 3.1). The number-average and weight-average molecular weights,  $M_n$  and  $M_w$  were found to be 5630 and 5726, respectively. The polydispersity index, PDI, was found to be 1.017.

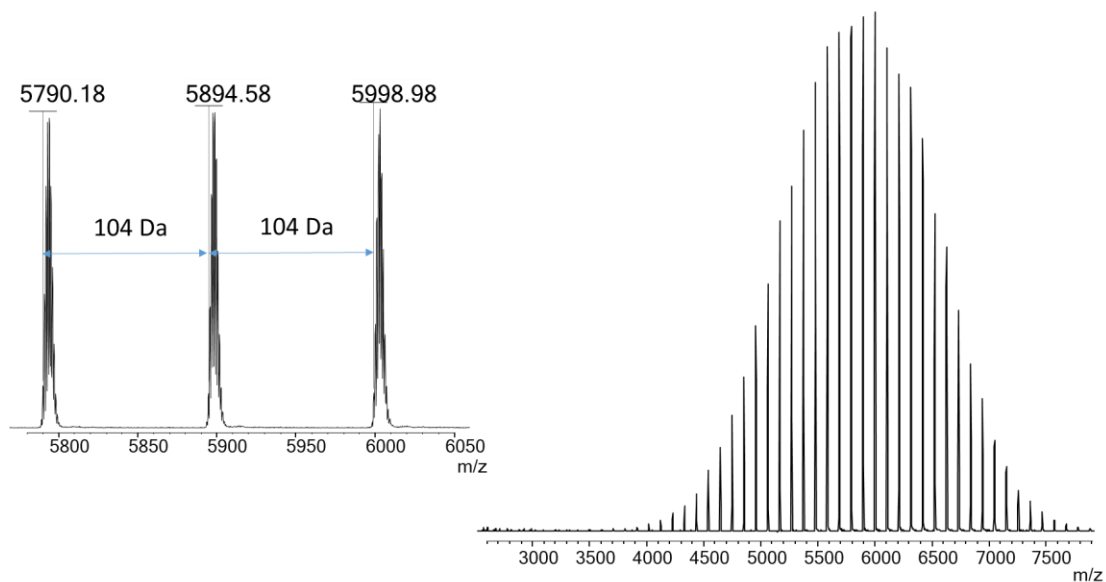


Figure **3.1**: Conventional bulk spectrum of the 6 kDa PS. The spectrum has a distribution from m/z of about 4000 to about 7700. The distribution indicates a repeat unit molecular mass of 104.4 Da.

For the SL-MALDI measurements for films, the matrix trans-2-[3-(4-tert-Butylphenyl)-2-methyl-2propenylidene] malononitrile (DCTB) and the cationization agent silver trifluoroacetate (AgTFA) were used, based on success with these in prior work.<sup>2-4</sup> DCTB with >98% purity was purchased from TCI, while AgTFA with >99.99% purity was purchased from Sigma-Aldrich. These materials were used as received.

### 3.2 Preparation of PS thin films

Pure 6k PS thin films for SL-MALDI MSI analysis were prepared by spin casting 1.5wt% PS solutions in toluene onto silicon wafers (Umicore, double side polished, 500-550  $\mu\text{m}$  thickness. 112 orientation). The sizes of the silicon wafers are 2 cm  $\times$  2 cm, which are chosen based on the size of the chuck of the spin coater as well as the size of the sample plate of the MALDI mass spectrometer. Before spin casting, each silicon wafer was cleaned in "piranha" solution (21ml  $\text{H}_2\text{SO}_4$  and 9 ml  $\text{H}_2\text{O}_2$ ) for 30 minutes to remove organic compounds, then rinsed with Milli-Q water and dried using compressed nitrogen. (*Warning: Piranha solution presents an explosion hazard and should be handled with extreme care; it is a strong oxidant and reacts violently with organic materials. All work should be performed in a fume hood. Wear proper protective equipment.*) PS films were formed after spinning at a rate of 2,000 rpm for 2 minutes.

The thicknesses of films were measured to be  $\sim 65\text{nm}$  using a spectroscopic ellipsometer (VASE, M-200 UV-visible-NIR [240-1700nm] J. A. Woollam Co., Inc., Lincoln, NE, USA). Analysis of the data were made assuming a model of four components: silicon wafer with a native oxide layer, a polymer film, and air. A polymer Cauchy model was used for polymer layers.

### 3.3 Two-step sublimation

Using an apparatus illustrated in Figure 3.2, matrix (DCTB) and ionization salt (AgTFA) were deposited onto the PS thin films by two-step sublimation. The sublimations conditions optimized by Guo's<sup>4</sup> are shown in Table 3.1.

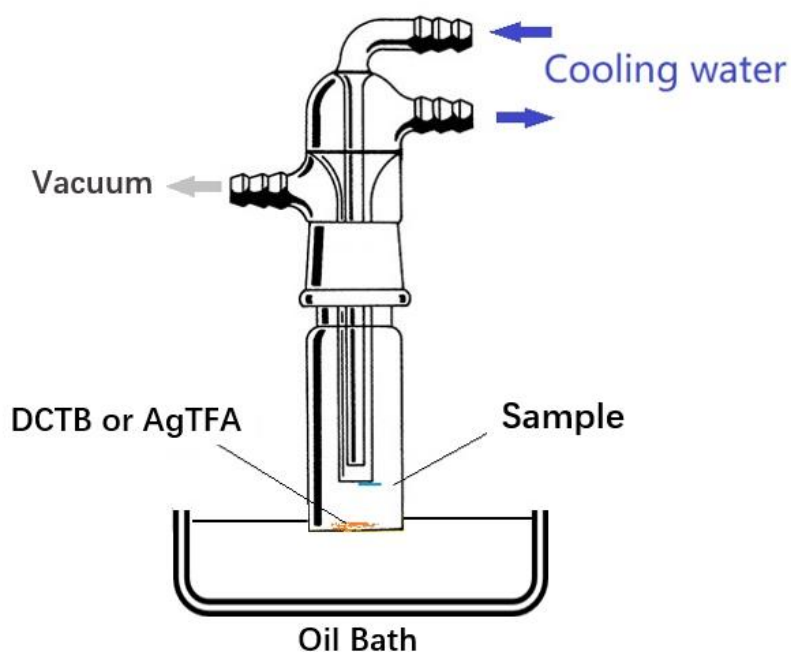


Figure 3.2: Schematic of sublimation apparatus.<sup>4</sup>

Table 3.1: Optimized conditions for two-step sublimation.<sup>4</sup>

	Amount	Temperature	Pressure	time
DCTB	50 mg	60°C	50 mTorr	40 min
AgTFA	50 mg	140°C	50 mTorr	40 min

By applying double-sided tape to the reverse side of each sample, the samples were attached to the bottom of the cold finger with the PS thin films side facing down. After adding matrix to the bottom of the chamber, the apparatus was sealed by evacuating the apparatus to 50 mTorr, as monitored by a vacuum gauge (Kurt J. Lesker Company<sup>®</sup> 205 A Series Thermocouple Gauge Controller). Before submerging the lower portion of the apparatus into the silicone oil bath, the setpoint of the solid-state recirculating chiller (ThermoTek Inc., T255P) was set at -5°C so that the temperature of the cooling water was maintained at 5-8°C during sublimation. In other words, the cooling bath was operating at the limit of its capacity, resulting in larger variations in cooling water temperature than should otherwise be achievable with this bath. The silicone oil was heated to the required temperature using a hot plate stirrer (Corning, PC-351) with feedback control and stirred constantly with a magnetic stirrer. After the pressure of the sublimation chamber and the temperatures of both the cooling water and oil bath reached the set points, the apparatus was lowered so that the bottom ~1 inch of the chamber was immersed in the oil bath.

Following sublimation, before opening the apparatus, the cooling water temperature was increased to ~20°C and kept at that temperature for around ten

minutes to prevent unwanted ice formation on the surface of the sample as a result of condensation on the cold finger and the cold sample surface. The sample was removed, the chamber cleaned, salt added into the chamber, and the sample reapplied and then the process above repeated for salt sublimation.

### 3.4 Characterization of samples

An atomic force microscope (Veeco Dimension Icon<sup>®</sup>, Bruker) was operated in tapping mode to characterize the morphology of the sample surfaces. MikroMasch HQ:NSC35/Cr-Au BS probes with cantilever force constant of 5.4 N/m and resonance frequency of 150 kHz (manufacturer's values) were used. After the sample was placed on the stage and held by a vacuum, the tip was engaged and tapped on the sample surface. The 5  $\mu\text{m}$   $\times$  5  $\mu\text{m}$  height sensor mode images were collected at three different spots for each sample after two-step sublimation. Since tapping mode was used phase signal images are obtained as well as height images. As is often the case in the AFM imaging of organic samples, variations in the morphology of the surface were more sharply evident in the phase images than in the height images. In particular, differences in morphologies of the crystals

formed could be observed. Contact mode AFM was also used to obtain the height sensor image of pure PS film surfaces.

Before SL-MALDI MSI analysis, optical images of samples were taken using an Epson Perfection 1670 Photo Scanner. Image resolutions were chosen according to the FlexImaging 2.1 User Manual Guidelines, in order to have the optical image resolution correspond to the desired MALDI image resolution. In this research, the resolution of the optical images was chosen to be 800 dots per inch (dpi).

SL-MALDI MSI was performed using a Bruker UltraFlex-III MALDI-ToF/ToF mass spectrometer (Bruker Daltonics, Billerica, MA) equipped with a neodymium-doped yttrium aluminum garnet (Nd/YAG) laser ( $\lambda = 355$  nm; 100 Hz repetition rate). The laser energy was adjusted to a proper intensity (50% of the full laser power) in order to avoid fragmentation of the polymer and minimize “bleed over” into adjacent raster spot regions. Before each measurement, the instrument was calibrated with a PS standard ( $M_n = 6.1$  kDa, PDI = 1.05; Scientific Polymer Products, Ontario, NY). The positive linear mode was used to maximize ion transmission and sensitivity. All spectra were measured by scanning the  $m/z$  range of 3000 to 8000 and 500 shots were accumulated at each raster spot. Since our



interest is the uniformity of signal intensity across the whole surface of a sample, three long rectangle regions consisting of approximately 180 raster positions per region were detected for each sample.

## CHAPTER IV

### RESULTS AND DISCUSSION

#### 4.1 Nonuniformity of the deposited layer

In the SL-MALDI images, the linear variation of the signal intensities from different pixels is shown using a gradient color scale. This gradient color scale directly corresponds to the variation of the concentration of a specific molecule. To visualize the molecular composition across the sample surface, a high fidelity is crucial for a reliable analysis. In other words, for a sample that is uniform in molecular composition across the surface, the colors, or signal intensities across the SL-MALDI image should be uniform.

The pure 6K PS films prepared by spin casting generally have smooth surface and uniform thickness. A tapping mode AFM image of a pure PS film sample is shown in Figure 4.1(a). The root mean square roughness of the scanned region is  $R_q = 0.489$  nm. However, after depositing matrix (DCTB) and

ionization salt (AgTFA) onto the surfaces of such uniform PS films using two-step sublimation and the optimized sublimation conditions, the obtained SL-MALDI images do not show uniform colors (Figure 4.2).

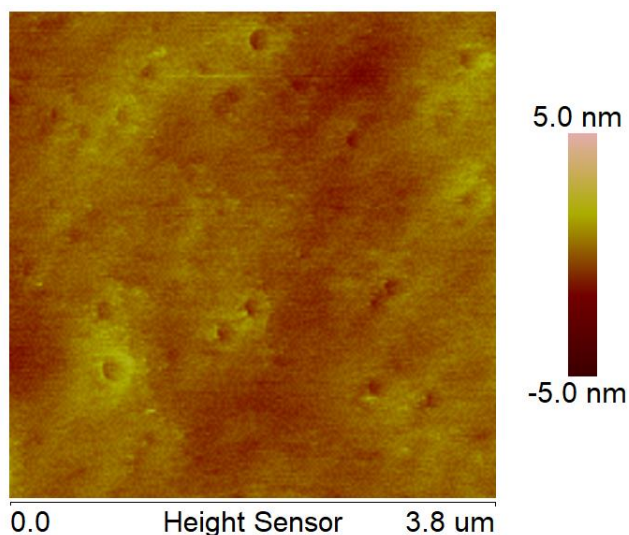


Figure 4.1: Tapping mode height sensor image of 6K PS film. The gradient of the color scale bar represents the height variation across the scanned region on the sample surface. The root mean square roughness obtained from this image is  $R_q = 0.489$  nm.

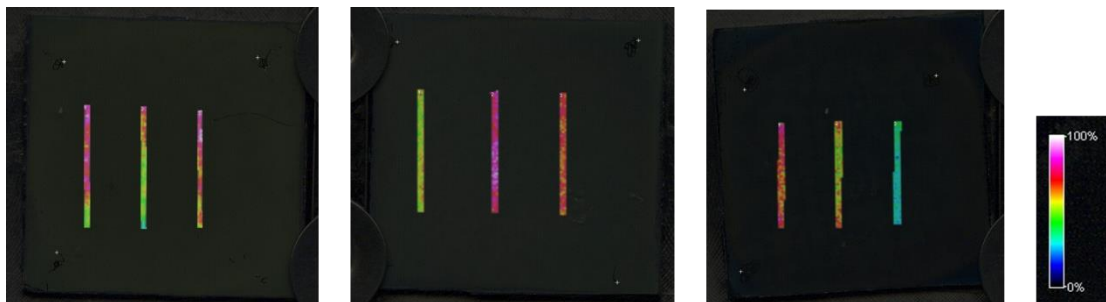


Figure 4.2: False color SL-MALDI images of three 6K PS thin film samples. For each sample, three long rectangular regions have been scanned. The gradient of color on the scale to the right of the image represents a linear variation in signal intensity and is based on spectra intensity relative to the highest intensity for the entire sample.

As shown in Figure 4.3(a-c), the height sensor images are obtained from three different regions of one sample after two-step sublimation using tapping mode AFM. A layer of matrix and salt was formed on top of the pure PS thin film layer for each sample after the two-step sublimation. These height images show the height variations of the matrix/salt layer on the sample surfaces within a range of  $-1\ \mu\text{m}$  to  $1\ \mu\text{m}$ . This quite large height range is required by the large apparent heights encountered in image (a). However, image (c) looks much more uniform than do images (a) and (b). Distinct outlines of portions of the surface are observed in images (a) and (b) are probably the outlines of crystalline regions within the imaged areas. Furthermore, these outlined regions in image (a) appear to be bigger than those in image (b). The height variations in image (c) are much smaller, so that they are not apparent with the scale used here. The character of the surface morphology is clearly quite different at different spots of one sample.

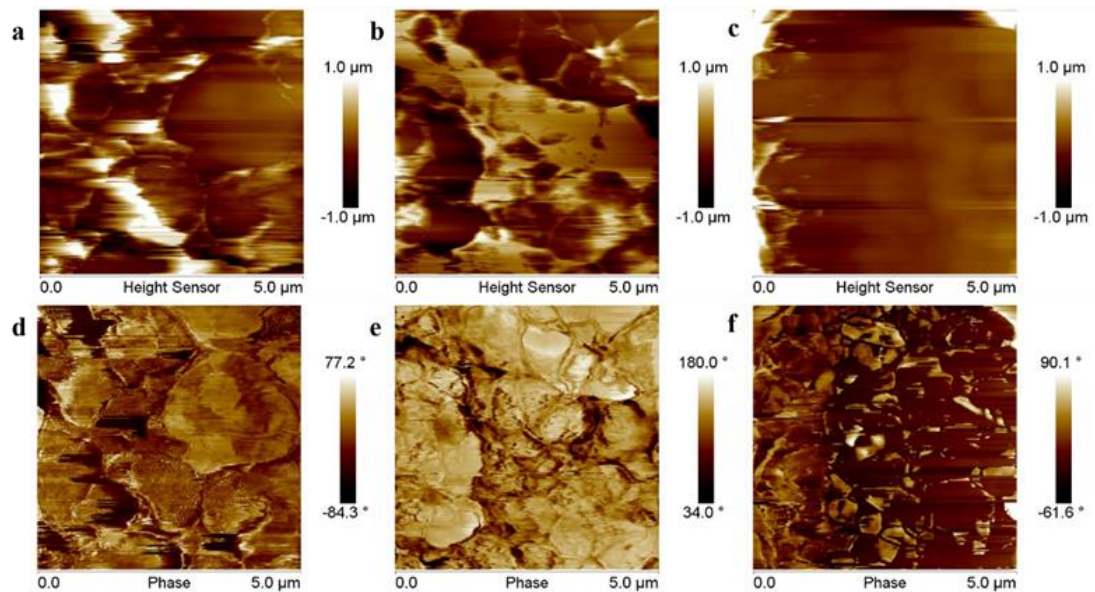


Figure 4.3: (a), (b) and (c) are tapping mode AFM height images from three different spots on one sample after two-step sublimation. (d), (e) and (f) are corresponding tapping mode AFM phase images collected simultaneously with (a), (b) and (c).

Phase images collected simultaneously with the height images are shown in Figure 4.3 (d–f). The phase images show more strikingly the changes in the surface morphology with change in position on the sample. Understanding what changes in phase mean is more difficult than interpreting differences in height. Such changes can result from changes in height, but also from changes in the mechanical properties of the material under the tip. In the current case, the changes in phase in the image could be due to material varying in height, or in some other way caused by the deposition of the salt on top of the matrix. The largest differences in phase appear in image (e). We suppose that these

differences in phase are related to the crystallization of DCTB. The details of the DCTB crystal structure are strongly influenced by the thermal conditions, particularly the temperature at which the crystals are formed and the local temperature during the salt deposition. When the hot salt condenses on the sample surface, the matrix layer that formed previously may be altered because the DCTB crystals have a melting temperature much below the temperature used to sublime the salt. The chief message from these images is that the surface morphology of the matrix and salt layer varies quite a bit with location on the sample, suggesting that the nature of the layer also varies strongly with position. These indications of lateral variation in the matrix and salt layer suggest indirectly that at the polymer interface with the matrix/salt layer, where the crucial polymer/matrix contact is made, the character of the deposited matrix/salt layer may likewise be strongly dependent on position.

There are some regions in the phase images showing very dark color, indicating that the tip was unable to actually tap on the surface because the height of these regions was too low (due to a deep hole) or the height was changing too rapidly for the force feedback mechanism to keep the probe touching the surface. The size and the number of these dark regions are also different for the three images. The nonuniformity of the matrix/salt layer could

strongly affect the signal intensity on the MALDI images. To improve the fidelity, it is crucial to deposit a uniform layer of matrix/salt onto sample surfaces.

## 4.2 Possible factors causing the nonuniform deposition

By looking at the details of sublimation apparatus and the sublimation process, several factors were believed to be responsible for the nonuniform deposition of matrix and ionization salt. One of the most obvious problems was that the cold finger in the apparatus had a concave bottom, whose shape was too curved for a 2 cm × 2 cm sample to be attached at the middle part of the cold finger bottom, as shown in Figure 4.4(a). When the sample could only be attached to the edge of the cold finger bottom, only a small part of the sample was actually contacting the bottom of the cold finger. Therefore, the cooling of the sample was far from uniform.

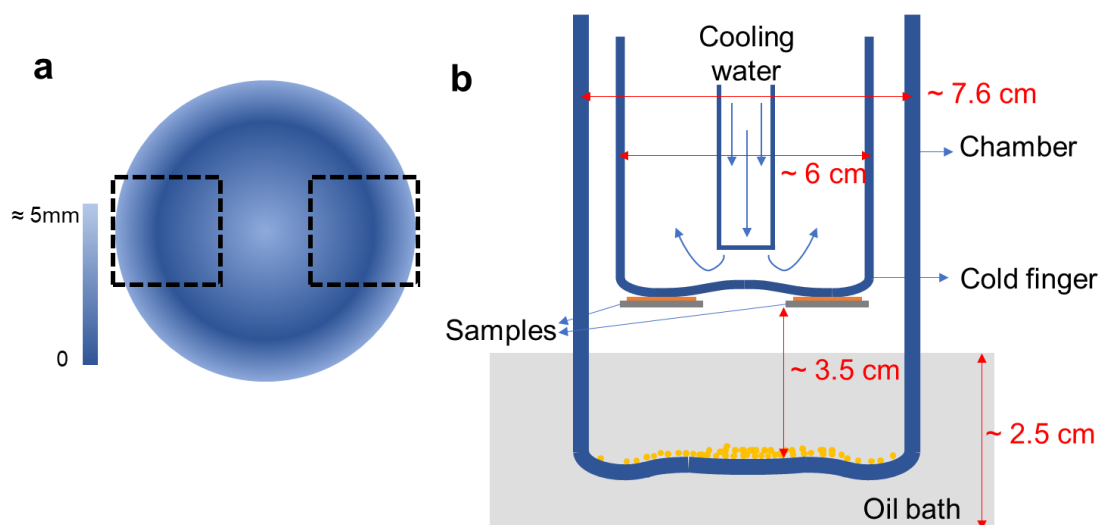


Figure 4.4: (a) Schematic showing the bottom up view of the cold finger bottom with two 2 cm x 2 cm samples attached to the edge. The gradient of the false color scale bar represents the vertical distance from the outer wall of the cold finger to the reverse face of the samples. (b) Schematic showing a cross section view of the lower parts of the cold finger and the chamber.

Due to the relatively small amount of matrix and ionization salt it is difficult to spread the matrix or ionization salt uniformly in the bottom of chamber. In previous work, matrix and ionization salt were put at the center of the chamber and spread by tapping the sides of the chamber gently. Examples of the distributions of matrix and ionization agent created in this regular way are shown in Figure 4.5, where the areal densities of matrix and ionization salt on bottom of the chamber are highest in the center of the chamber. However, since the samples were attached to the edge of the cold finger bottom, the sample surfaces were not directly facing the part of chamber bottom with the highest



areal densities of matrix or salt. In addition, as shown in Figure 4.4(b), the chamber in the apparatus had a thick wall and a curved shape at the bottom, adding to the difficulty in distributing and heating the matrix and salt uniformly.

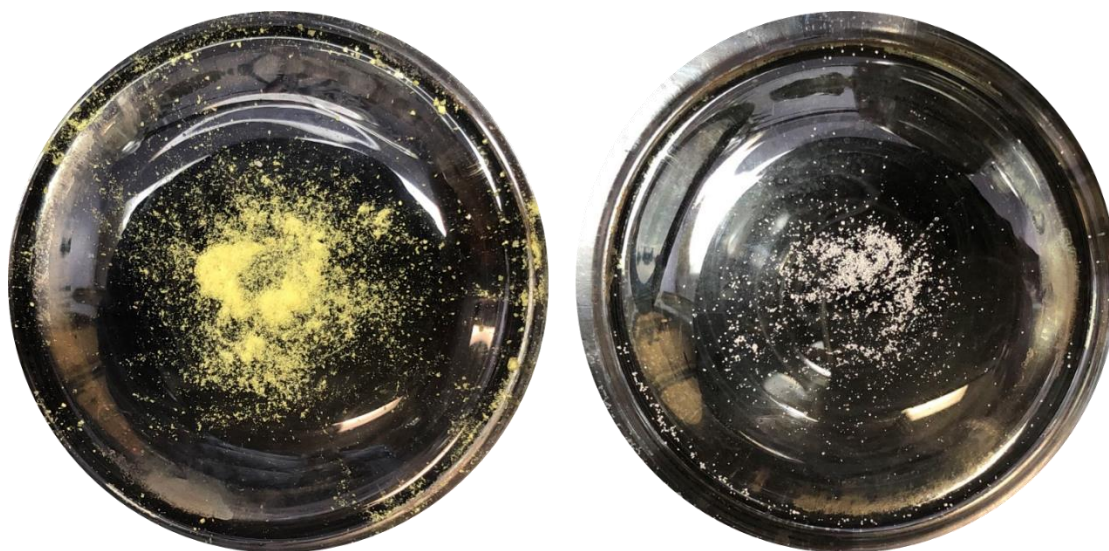


Figure 4.5: The distribution of 50 mg DCTB (left) and 50 mg AgTFA (right) at the bottom inside of the chamber creating by the regular operation.

Overall, there are several factors that could lead to nonuniformity in the deposited layer. Although the lateral variations in the sample temperature across the sample surface and in the matrix/salt temperature across the chamber surface could play an important role, the nonuniformity could also be influenced by the distribution of matrix and salt in the chamber. Therefore, the effects of the distributions of matrix and salt were investigated next.

### 4.3 Investigation on distributions of matrix and salt

By putting the matrix or ionization salt directly beneath one of the two samples attached to the cold finger and thus diagonally below the other sample, the influence of the distribution of matrix or ionization salt can be determined by comparing images acquired from SL-MALDI-TOF MSI analysis. These different ways of distributing the matrix and salt are illustrated in Figure 4.6 and the conditions for the analyses of five samples are listed in Table 4.1.

Table 4.1: Distribution of matrix and salt investigated

<b>Samples</b>	<b>Matrix distribution</b>	<b>Salt distribution</b>
1	Regular	Regular
2	Opposite of the projection of the sample	Regular
3	Right beneath the sample	Regular
4	Regular	Right beneath the sample
5	Regular	Opposite of the projection of the sample

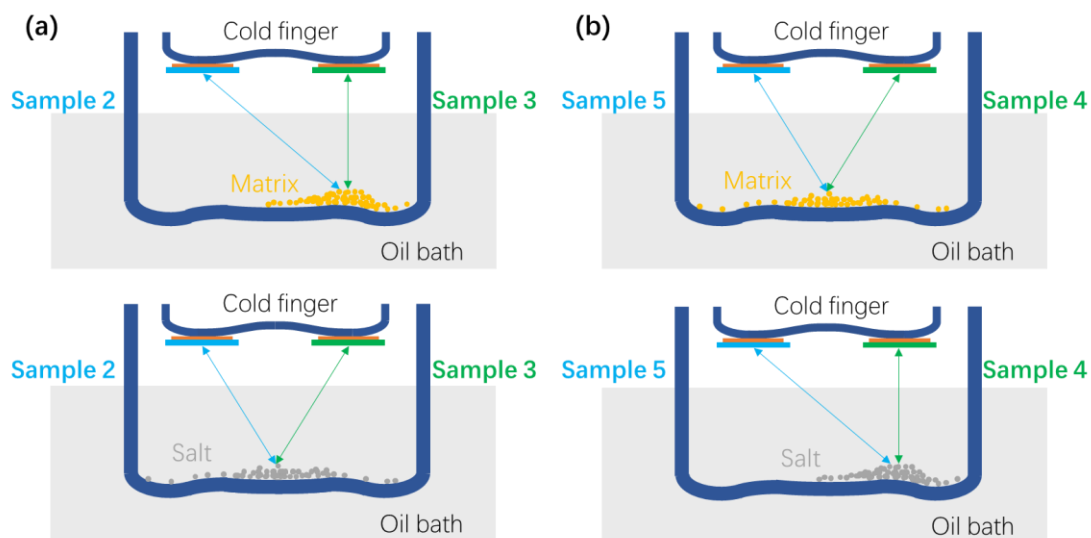


Figure 4.6: Schematic showing the distributions of matrix and salt for different samples. (a) Distributions for Samples 2 and 3, for which the matrix travels a much shorter path length to get to the surface of Sample 3 than to the surface of Sample 2, while the salt travels for a similar path length to get to the surfaces of the two samples. (b) Distributions for Samples 4 and 5, for which the salt travels a much shorter path length to get to the surface of Sample 4 than to the surface of Sample 5, while the salt travels for a similar path length to get to the surfaces of the two samples.

#### 4.3.1 Matrix distribution

When comparing the SL-MALDI images of samples made using different matrix distributions, some differences in the signal intensity were observed.

Figure 4.7 shows the SL-MALDI image of a sample made with regular distributions of matrix and ionization salt, as well as the spectrum of one pixel selected from the SL-MALDI image. Figure 4.8 shows the SL-MALDI images and

spectra of two samples prepared simultaneously, one of which was placed right over the matrix and the other of which was attached to the opposite side of the cold finger.

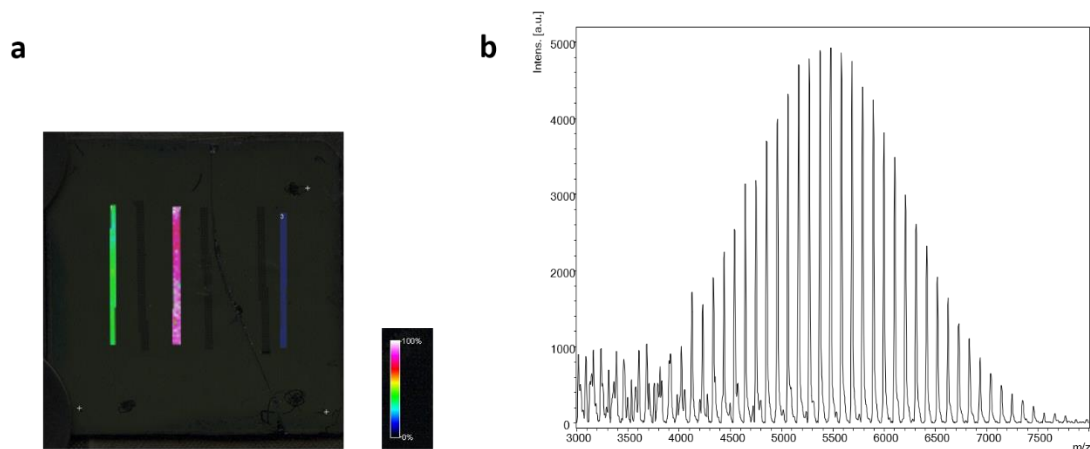


Figure 4.7: (a) SL-MALDI image of sample 1 which was prepared by two-step sublimation with regular distributions of both matrix and ionization salt. (b) Spectrum of one pixel with the highest intensity selected from the SL-MALDI image in (a).

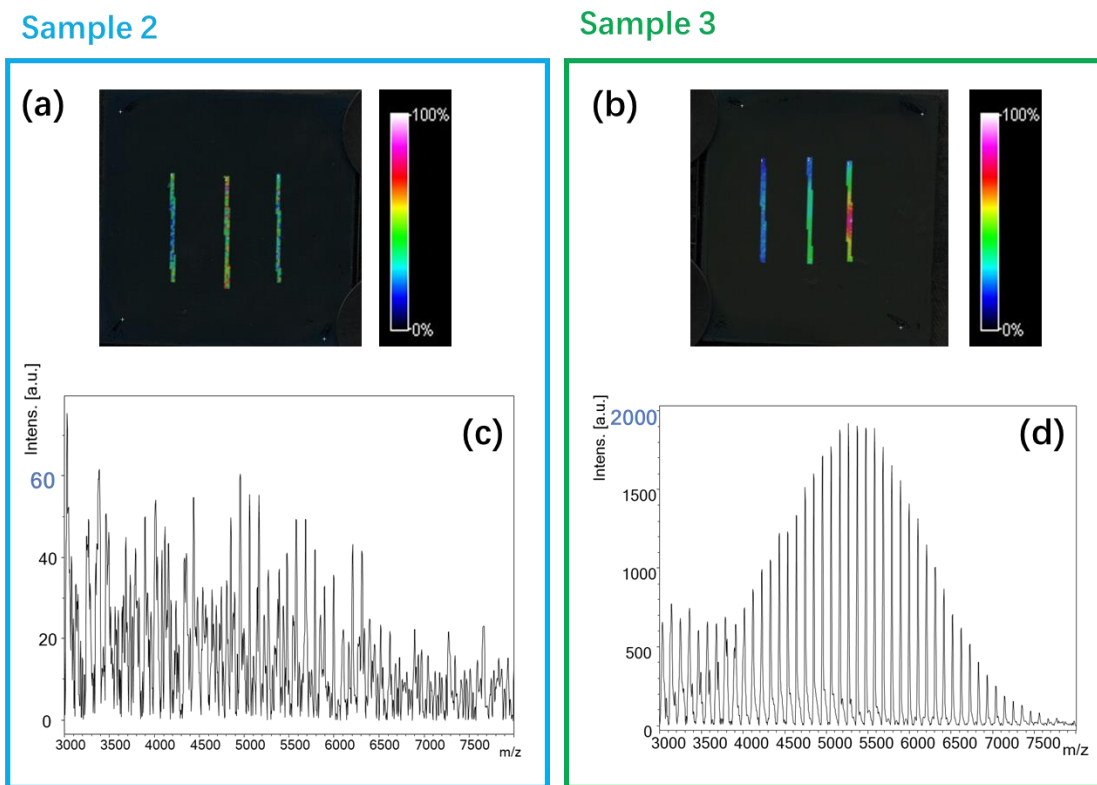


Figure 4.8: (a) and (b) are the SL-MALDI images of two samples prepared simultaneously with regular distribution of ionization salt, but with different distributions of matrix. Sample 3 with matrix right beneath it gave the image in (b), while Sample 2 attached on the opposite edge of the cold finger gave the image in (a). (c) and (d) are the spectra of one pixel with the highest intensity selected from the SL-MALDI images in (a) and (b), respectively.

Comparison of the images indicated that the placement of the samples in relation to the distribution of the matrix has an influence on the overall signal. The image of the sample placed far away from the majority of matrix shows overall low intensity, leading to a spectrum which gives little useful information due to the background noise.

However, the spectrum acquired from the Sample 3, which was made with matrix distributed right beneath it, as shown in Figure 4.8(b) looks similar to the one acquired from the sample made with regular distribution of both matrix and salt, as shown in Figure 4.7(b). However, the overall intensity of the former spectrum is lower than that of the latter. Both spectra show a clear distribution of 6K PS with the base peak shifted to a smaller  $m/z$  value compared to the spectrum of bulk PS as shown in Figure 3.1. This is caused by the preference for smaller chains at the surface of homopolymer films due to an entropic effect on the film's overall free energy.

#### 4.3.2 Salt distribution

The contrast between the two samples made with different distributions of salt appears to be more drastic than the contrast between those made with different matrix distributions. As shown in Figure 4.9(c), the SL-MALDI image of Sample 5 which was placed far away from most of the salt in the chamber shows overall poor signal corresponding to a spectrum with almost completely background noise. In contrast, the SL-MALDI image shown in Figure 4.9(b) for the sample prepared with salt directly underneath shows some regions with

relatively high signal intensity, from where a valuable spectrum showing the distribution of 6K PS thin film can be acquired.

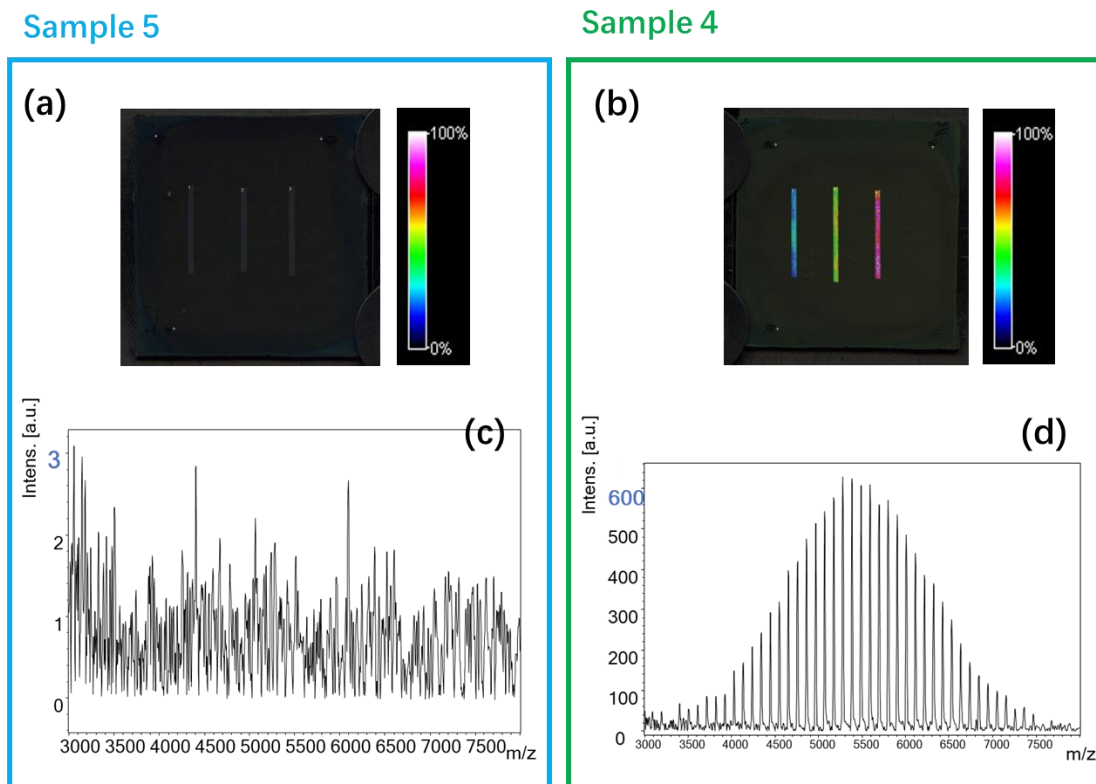


Figure 4.9: (a) and (b) are the SL-MALDI images of two samples prepared simultaneously with regular distribution of matrix, but with different distributions of ionization salt. The sample with salt right beneath it gave the image in (b), while the sample attached on the opposite edge of the cold finger gave the image in (a). (c) and (d) are spectra of one pixel with the highest intensity selected from the SL-MALDI images in (a) and (b), respectively.

It is obvious that the salt distribution seems to have more effect on the quality of the SL-MALDI images than does the matrix distribution. One possible factor causing this is that AgTFA is a more densely packed crystal than DCTB,

which is loose and powdery at room temperature. Since 50 mg of each compound is used during the two-step sublimation, the DCTB spreads better and covered more of the bottom chamber than AgTFA did. Another possible explanation is that the sublimation temperature for salt is much higher than that for matrix, which makes the path length between salt/matrix and sample surface play a bigger role.

#### 4.4 Elimination of thermal gradients

In the investigation on the effects of distributions of the matrix and ionization salt, the nonuniformity of the signal intensities across the PS sample surfaces was not improved by moving most of the matrix or ionization salt to the position right under the surface of the sample. Therefore, it can be concluded that the distributions of matrix or salt alone cannot cause such nonuniformity in signal intensity and that the thermal gradients existing in the cooling of the sample and in the heating of the matrix/salt are more responsible for the nonuniformity.



#### 4.4.1 Efforts in eliminating thermal gradients

The most significant changes are the modification of the cold finger bottom and the rebuilding of the chamber bottom. The schematics of these two parts after reshaping are shown in Figure 4.10. Compared to the apparatus before the reshaping, which is shown in Figure 4.4, the bottom of the cold finger becomes relatively flat, so that a 2 cm × 2 cm sample can be attached to the middle, with a much larger part of the sample coming in direct contact with the cold finger. This change greatly reduced the thermal gradient of the cooling to the sample. To ensure an even higher efficiency in the heat conduction between the cold finger wall and the sample, the regular double-sided tape (Scotch® permanent double-sided tape) was replaced by an electrically conductive double-sided tape.

The chamber wall at the bottom becomes slightly thinner and its shape becomes relatively flat after rebuilding, providing a better heat conduction between the silicon oil bath, the wall of the chamber and the matrix or salt inside of the chamber, and therefore reducing the thermal gradient of the heating to matrix or salt.

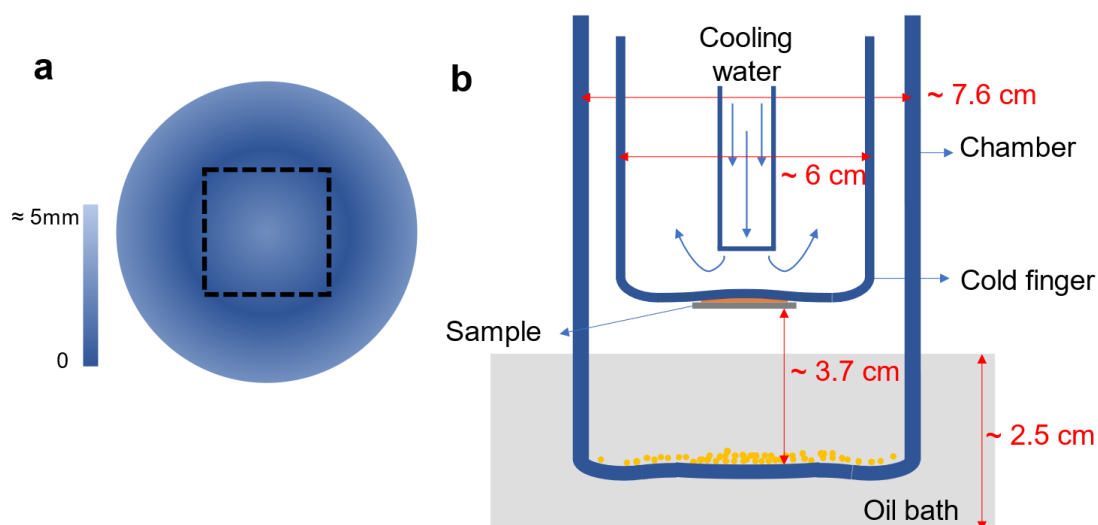


Figure 4.10: (a) Schematic showing the view looking up at the modified cold finger bottom with one 2 cm × 2 cm sample attached to the middle. The gradient of the false color scale bar represents the vertical distance from the outer wall of the cold finger to the back face of the sample. (b) Schematic showing the vertical cross section view of the lower parts of the modified cold finger and the rebuilt chamber.

For a closer contact between the chamber wall and the matrix<sup>23</sup>, a pretreatment to the matrix was incorporated by preparing a matrix film inside of the chamber using solvent evaporation method. Before every matrix sublimation, a desired amount of the matrix is dissolved in 10 mL of acetone. The volume of the acetone is chosen to cover the whole bottom area of the inside chamber because the bottom of the chamber is still not perfectly flat after rebuilding. A weak vacuum is applied to the apparatus so that the acetone can evaporate rapidly under room temperature, leaving a matrix film in the chamber. An example of the matrix films prepared using this method is shown in Figure 4.11.

The areal density of matrix is much more uniform than that prepared in a regular way, which is shown in Figure 4.5. With the matrix pretreatment, the thermal gradient in the heating of the matrix is further reduced.

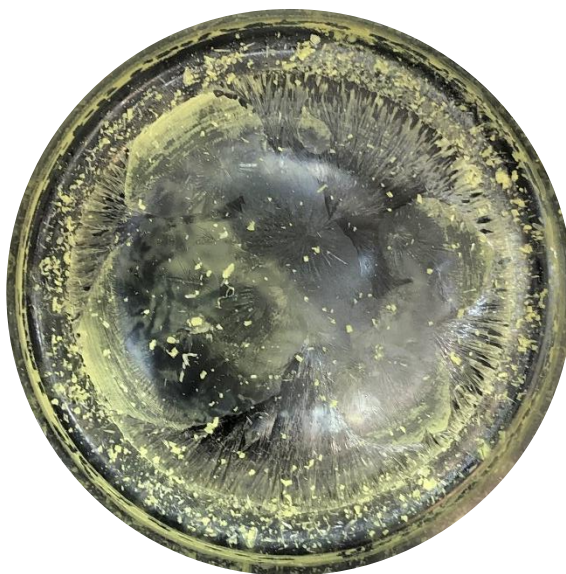


Figure 4.11: A matrix layer prepared from 50 mg of DCTB using the solvent evaporation method.

#### 4.4.2 Results of eliminating thermal gradients

After all the efforts in eliminating the thermal gradients described above were completed, several samples with unprecedented, good signal uniformity were acquired. The SL-MALDI images of two of those good samples are shown in Figure 4.12. The colors in these images are mostly pink and white, which are the colors closed to the end of 100% in the false color scale bar, corresponding

to high relative signal intensity. Compared to the SL-MALDI images shown previously, the uniformity has been greatly improved.

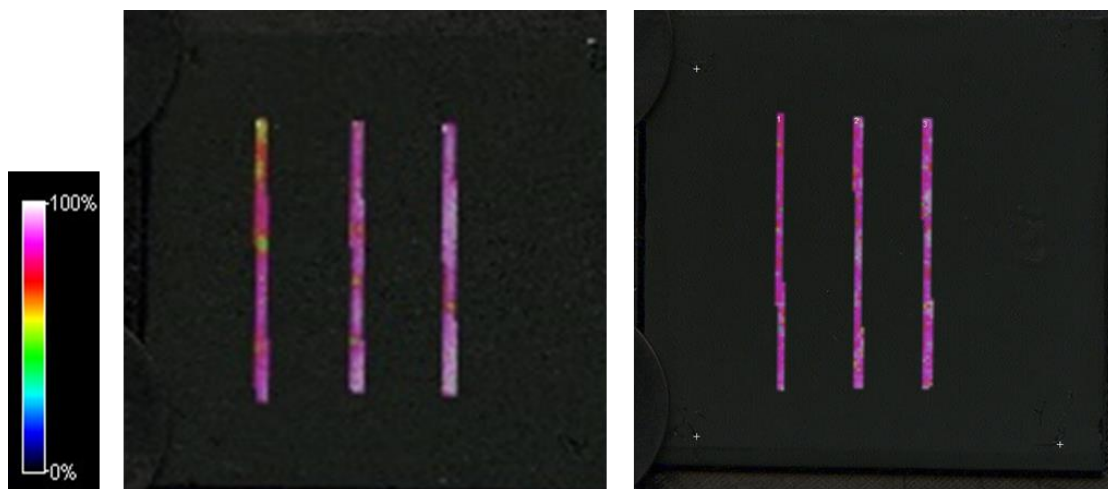


Figure 4.12: SL-MALDI images of two of the good samples obtained after all efforts of eliminating the thermal gradients were done.

However, the maximum signal intensities measured from each sample and the reproducibility of the technique still remain unsatisfactory. Some of the samples prepared using the same conditions do not give uniform signal intensities across the surfaces. In addition, as shown in Figure 4.13, a secondary distribution appears in the mass spectra occasionally. The spacing of the peaks in this secondary distribution is around 108 Da, which correspond to the atomic mass of silver. Therefore, the secondary distribution is assigned to the silver salt clusters. To ensure a reliable and convenient analysis process in future application using SL-MALDI MSI to characterize different materials, it is

necessary to improve the maximum signal intensity and the reproducibility, as well as to avoid the forming of the salt clusters. Although the exact reasons causing these limitations are unclear, it is almost certain that the sublimation conditions need further optimization.

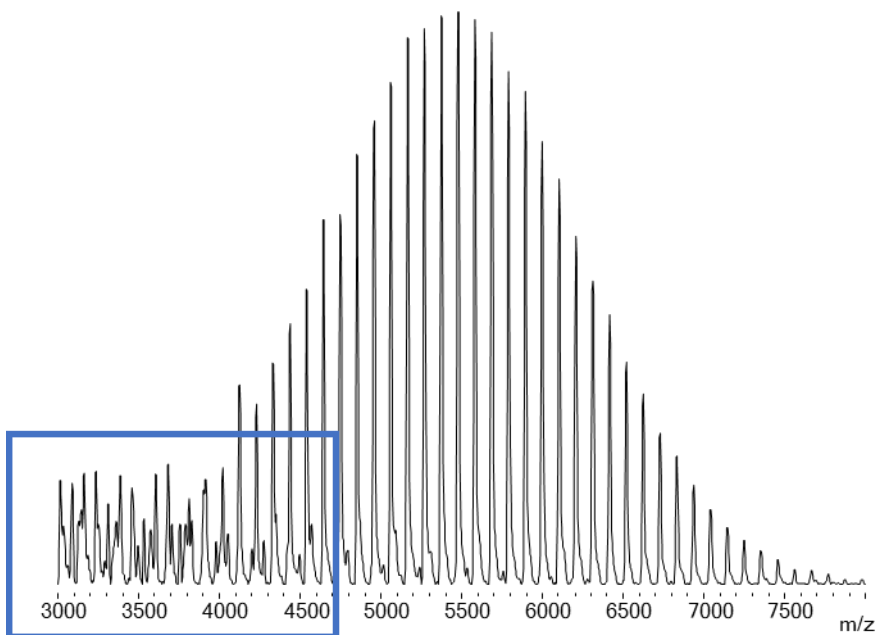


Figure 4.13: Mass spectrum corresponding to one pixel from the SL-MALDI image measured for one of the samples. The primary distribution is the mass distribution of 6K PS, with a spacing of  $\sim 104$  Da. The secondary distribution shown in the blue box corresponds to the mass distribution of the sliver salt clusters.

## 4.5 Optimization of sublimation conditions

### 4.5.1 Matrix/salt amount and sublimation time

In a sublimation process, there are many variables that could affect the sublimation quality, including the temperature of the oil bath and cooling water, the pressure, the amounts of matrix and salt in the chamber, and the sublimation time. In this section, the optimized heating temperatures for matrix and salt provided by Guo<sup>4</sup> (listed in Tale 3.1) were used. The pressure was kept within 40-60 mTorr during sublimation. The sublimation time was the same for matrix and salt sublimation. A certain amount of matrix was used to prepared matrix layer before matrix sublimation, while the same amount of salt powder was directly added into chamber before salt sublimation. Six groups of samples were prepared using the different conditions listed in Table 4.2.

Table 4.2: Sublimation conditions investigated for S1-S6.

Group No.	Amount (mg)	Sublimation time (min)
S1	50	40
S2	40	40
S3	30	40
S4	40	30
S5	40	20
S6	40	50

Among the samples prepared using the six different groups of sublimation conditions, good uniformity of signal intensities always occurred for the samples prepared using condition group S2, where matrix amount and salt amount were both 40 mg and the sublimation times were both 40 min for each step. The SL-MALDI images of one sample from each group are shown in Figure 4.14. It is obvious that the image in (b) has the most uniform signal intensities. The image in (f) also shows good signal uniformity, but the maximum signal intensity from this group is too low to ensure a reliable analysis.

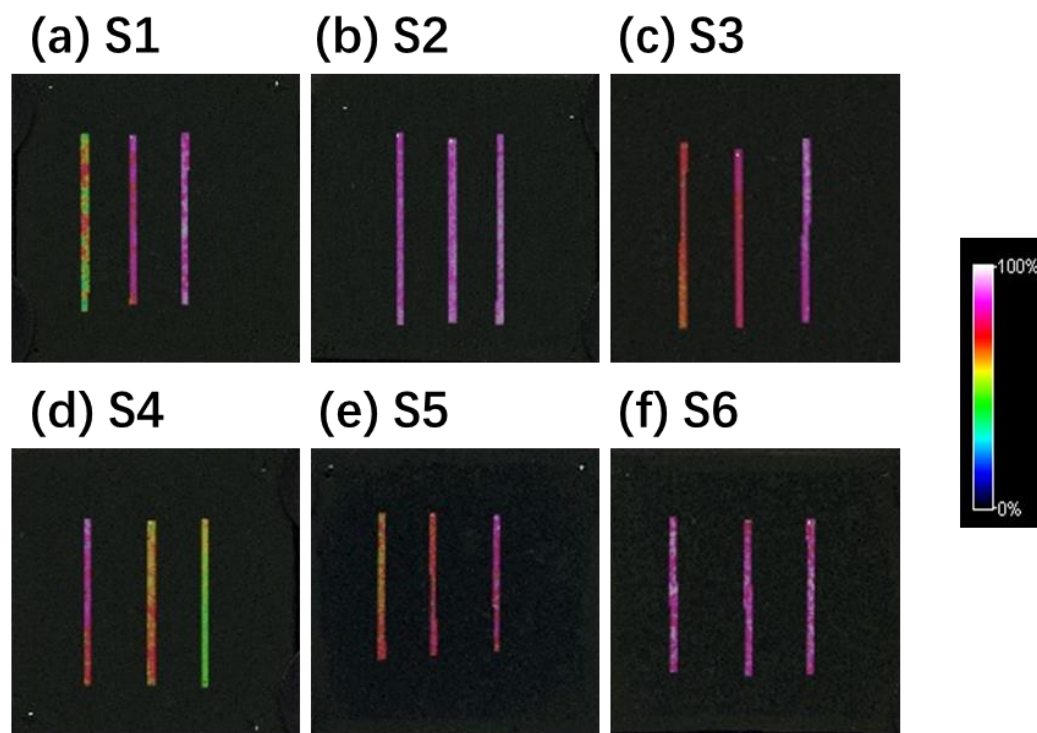


Figure 4.14: SL-MALDI images of samples from group S1 (a), S2 (b), S3 (c), S4 (d), S5 (e) and S6 (f).

To verify whether the results of the samples prepared using the condition group S2 were reproducible, several samples were prepared using the same conditions. Unfortunately, the good signal uniformity is not consistent, as shown in Figure 4.15, where the variability in the color gradient changes quite a bit across the surface of each sample.

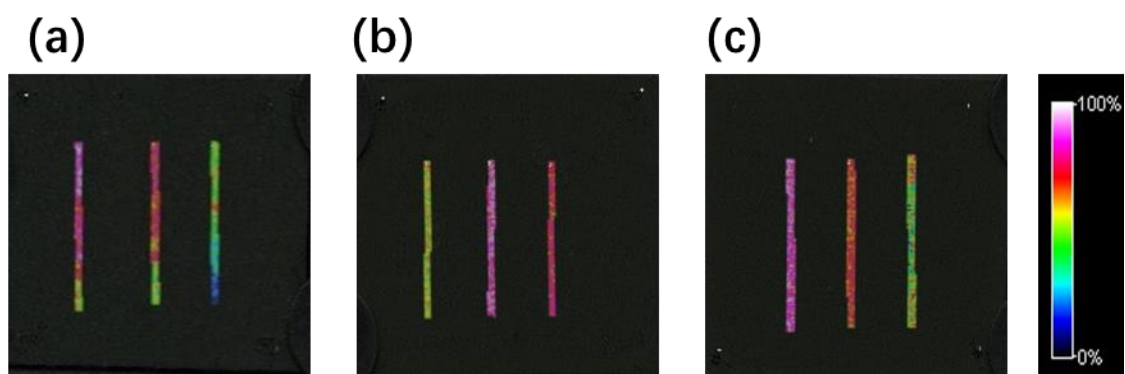


Figure 4.15: SL-MALDI images of three samples prepared using the conditions in group S2. The signal intensities are much less uniform than those in Figure 4.14(b).

In addition to the inconsistent uniformity of signal intensities, the appearance of the secondary mass distribution resulting from salt clusters is not consistent either. No signal from salts was detected for the samples shown in Figure 4.14(b) and Figure 4.15(a). In contrast, distinct salt signals were detected across the surface of the sample in Figure 4.15(b). For the last sample in Figure 4.15(c), very weak salt signals were detected from only a few pixels. This occasional appearance of salt clusters could be caused by too much salt



deposited onto the sample surfaces. Another possible reason is that the salt could be deposited onto sample surface nonuniformly, forming salt clusters in only some regions of the sample surface. What's more, the random appearance of salt clusters could be one of the factors affecting the reproducibility of the signal uniformity.

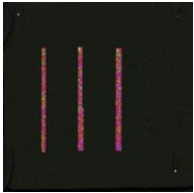
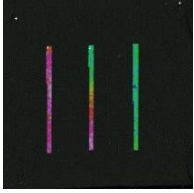
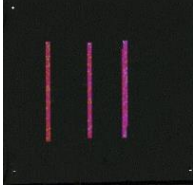
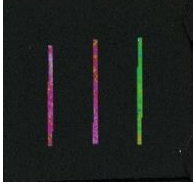
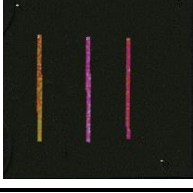
#### 4.5.2 Elimination of salt clusters

In the trials of eliminating the appearance of salt clusters, several samples were prepared with less salt deposited on the surfaces (Table 4.3). The reduced amounts of deposited salt were achieved by reducing the amount of salt added into chamber (C1 and C2), decreasing the heating temperature during salt sublimation (C3 and C4), or shortening the time for salt sublimation (C5). Other conditions during the two-step sublimation for these samples were the same as those for the sample in group S2.

The results show that salt clustered appeared in all samples except C4, which however, did not show uniform signal intensity. C1 and C3 gave relatively uniform signal intensities but also distinct salt distributions in mass spectra. Therefore, by reducing the amount of deposited salt on sample surfaces alone,

none of the samples were free of the salt clusters and gave good uniformity at the same time.

**Table 4.3:** Conditions of salt sublimation and results for samples C1-C5.

Sample	Salt sublimation conditions			Salt clusters	Results
	Amount (mg)	Time (min)	Temp. (°C)		SL-MALDI image
C1	30	40	140	Yes	
C2	20	40	140	Yes	
C3	40	40	130	Yes	
C4	40	40	120	No	
C5	40	30	140	Yes	

#### 4.5.3 Necessity of salt pretreatment

From the above experiments aiming at improving the reliability of the technique by adjusting the sublimation conditions, it appears that there is still a strong inconsistency in the SL-MALDI results. Here, a speculation could be made that a proper pretreatment for the ionization salt is necessary for reproducible, good fidelity of the technique.

According to the investigation of the effects of matrix/salt distributions described in previous section 4.3, the salt distribution has a stronger effect on the quality of SL-MALDI images than does the matrix distribution, which is due to the higher mass density of AgTFA powder and the higher heating temperature used in salt sublimation. In addition, the morphology and roughness of the sample surface are definitely changed by the salt deposition, as the matrix melts when contacting the hot sublimated salt molecules, leading to the formation of matrix/salt co-crystals.

In the above experiments, there was no salt pretreatment before salt sublimation for any samples. Instead, the salt powder was distributed in a regular way, where the areal density of salt was the highest at the middle of the chamber and was far from uniform across the bottom of chamber. This nonuniform source

of salt could contribute to the nonuniform deposition of salt. Furthermore, since the control over the salt distribution was poor, the distribution of salt varied from sample to sample, which could increase the variation of the deposition quality.

The changes in surface morphology of the sample before and after salt deposition provide evidence for the necessity of salt pretreatment. Figure 4.16(a-b) shows the  $10\ \mu\text{m} \times 10\ \mu\text{m}$  height sensor images of the sample surfaces before and after salt deposition measured using tapping mode AFM. The false color scale bars representing the height variations across the scanned region, are the same for the two images. In the image obtained from sample after salt deposition, the contrast is stronger, with more dark and bright regions across the surface. The outlined regions in the height images correspond to the crystal morphology at the surfaces. It is clear that the sizes and the shapes of the matrix crystals are similar in image (a). In contrast, the matrix/salt co-crystals have various shapes and sizes across the surface in (b).

In Figure 4.16(c), the height variations along the section lines in the two AFM height images are plotted together. The heights along the section from the sample with the matrix/salt layer at the surface vary from above  $+0.5\ \mu\text{m}$  to below  $-0.5\ \mu\text{m}$ , while the range of height variations is much smaller for the sample without salt deposition. In addition, the root mean square roughness of the

images obtained before and after salt deposition are 148 nm and 272 nm, respectively. Hence, as the surface roughness increases during the salt deposition, the sample surfaces become much less uniform.

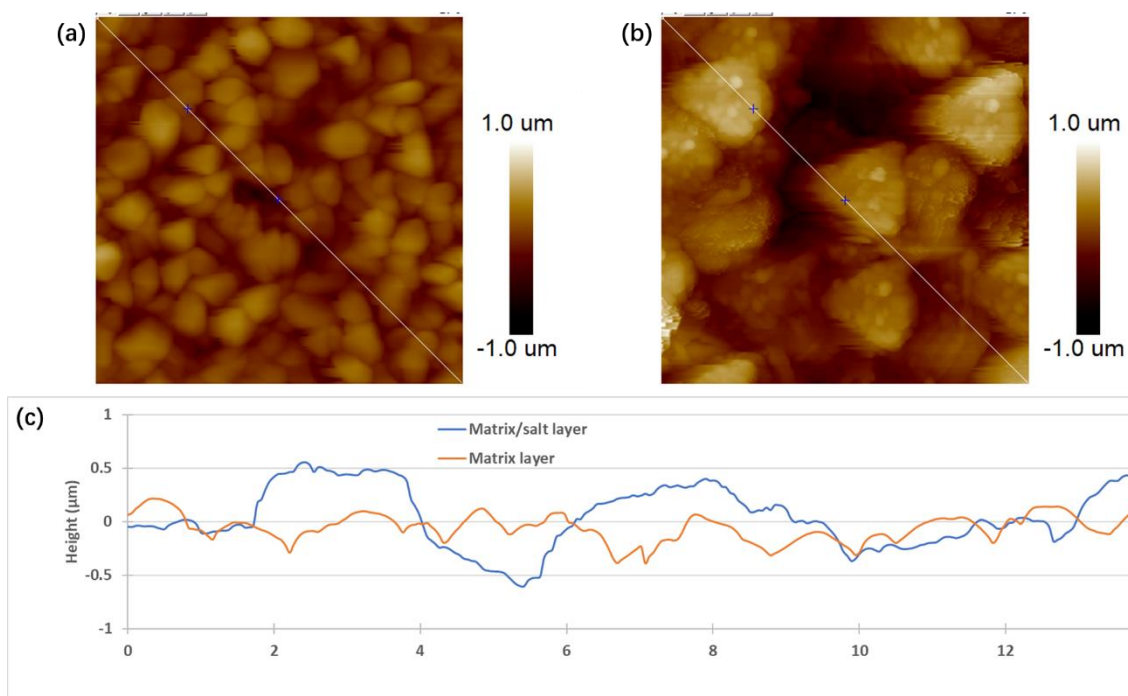


Figure 4.16: (a) 10 μm × 10 μm height sensor image measured by tapping mode AFM from a sample with only matrix deposited on the surface. The root mean square roughness obtained from this region is  $R_q = 148$  nm. (b) 10 μm × 10 μm height sensor image measured by tapping mode AFM from a sample after salt deposition with a  $R_q = 272$  nm. (c) The height variations along the section lines in (a) and (b).

Another evidence is that the form of the salt powder used as the salt source in salt sublimation influences the quality of SL-MALDI images significantly. Figure 4.17(a) and (b) show the distributions of 40 mg of two different AgTFA salt products in the chamber, a closer view of the middle part of

which is provided in (c) and (d), respectively. In our experiments, it is found from the samples prepared using the salt powders shown in (a) that there is a much higher probability of obtaining generally low signal intensity and distinct signals from salt clusters, while the samples prepared using salt powders shown in (b) are more likely to give uniform signal intensity. This difference could at least partly result from the difference in the form of the salt powders. The salt powders shown in (b) are much finer crystals compared to those in (a) and therefore can spread out more easily. It is also possible that salt powders with different forms experience different melting and sublimating behavior during the sublimation process.

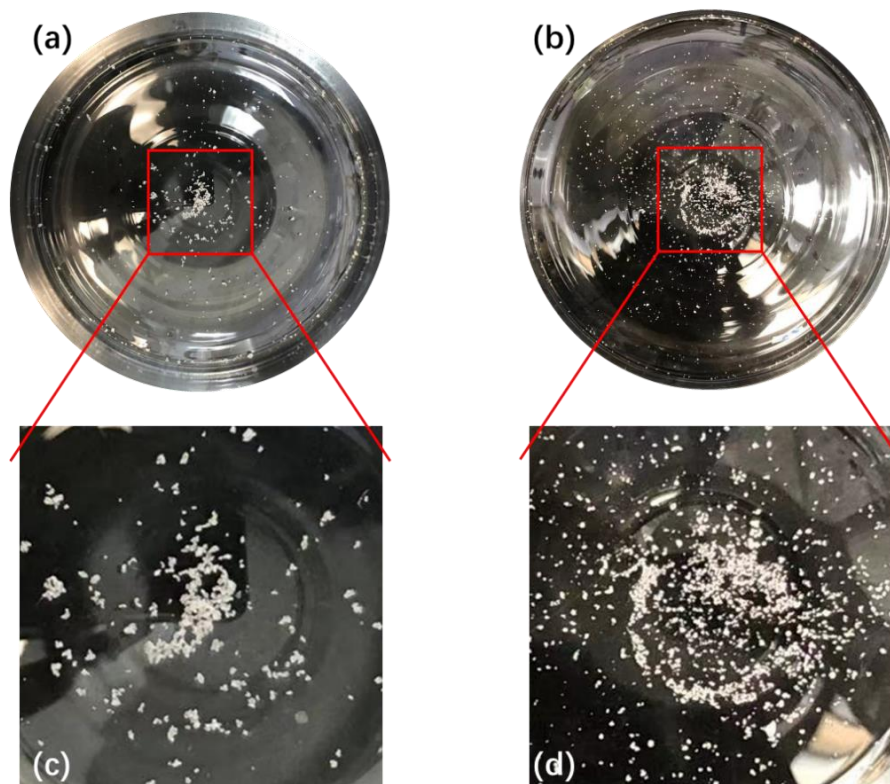


Figure 4.17: (a) and (b) are the photographs showing the distributions of 40 mg of two AgTFA salt products in chamber. (c) and (d) are the zoom-in views of the middle parts in (a) and (b), respectively.

In conclusion, it is necessary to carry out the proper pretreatment of the salt before salt sublimation to ensure a uniform salt deposition. Here, we propose a possible solution by preparing a salt film on a separate substrate, which can be attached to the middle of the inside chamber bottom using thermally conductive tape and used as the salt source during salt sublimation. Using methods such as the solvent evaporation method, a salt film with more uniform areal density of salt can be formed.

## CHAPTER V

### CONCLUSION

Two-step sublimation is the best choice for preparing samples for SL-MALDI MSI analysis, but the apparatus and preparation process still need to be improved in order to acquire consistent and reproducible results. Solving the nonuniformity of signal intensity of SL-MALDI images obtained from samples with uniform molecular composition across the surfaces is the main focus of this work.

In this research, the influences of the distributions of matrix and ionization salt in the sublimation chamber on the lateral uniformity of sample intensity were first investigated. It can be concluded that the distributions of both matrix and ionization salt have some effect on the lateral uniformity of MALDI images of laterally uniform surfaces and therefore on the fidelity of composition imaging in samples with laterally nonuniform compositions. To acquire acceptable MALDI images with high fidelity and high signal intensity, the matrix and ionization salt should be placed near the projection of a sample on the bottom of the chamber.



An increased deposition path length between a sample and either matrix or salt can lead to images with overall low intensity in which background noise significantly interferes or even overwhelms the signal. In particular, the ionization salt distribution has a greater influence on MALDI images than does the matrix distribution, which could be related to the greater difficulty in spreading the salt as uniformly as the matrix in the bottom of the chamber, or to the significantly higher temperature to get the salt to sublime.

However, even when moving the majority of matrix or ionization salt directly under the sample onto which they are being sublimated, some lateral nonuniformity of signal intensity still remained. Hence, the thermal gradient that exists as a result of the concave shape of the bottom of the cold finger now becomes more suspect as the main factor causing the nonuniform signal intensity. In addition, thermal gradients also occur in the heating of the matrix and salt due to the curved shape and wall thickness at the bottom of the chamber, as well as the nonuniform distributions of matrix and salt.

To eliminate the thermal gradients in the cooling of the samples and in the heating of the matrix/salt, several changes were made to the apparatus and the sublimation process. These changes included reshaping the bottoms of the cold finger and chamber, changing the matrix source from matrix powder to a matrix

film in the chamber and replacing the regular double-sided tape with thermally conductive double-sided tape to attach samples to the cold finger. As a result of these changes, the probability of obtaining high-quality SL-MALDI images from samples prepared by two-step sublimation significantly increases. However, the reproducibility remains unsatisfactory and the overall signal intensity needs further improvement. Furthermore, a secondary distribution resulting from sliver salt clusters appears in the mass spectra occasionally, which will affect the reliability of the analysis in future applications.

From the trials made in optimizing the sublimation conditions to improve the reproducibility and overall intensity and eliminate the appearance of salt clusters, we found that 40 mg of matrix and 40 min matrix sublimation time appear to give the most uniform deposition for the current setup and procedure. However, the signal uniformity and the appearance of salt clusters remain inconsistent, leading to a low reproducibility of the technique. From the observations that the samples show a rougher surface after salt sublimation, with much less uniform crystal sizes and shapes, and from the fact that the form of the salt powders strongly influences the quality of SL-MALDI images, we infer that the nonuniform salt source and the experiment-to-experiment variations in salt distribution are two of the main reasons leading to the low reproducibility after eliminating thermal gradients. Therefore, by

using a proper pretreatment of the salt, potentially the reproducibility can be improved. A proposed possible solution is to use as the source of salt sublimation a salt film on a separate substrate attached to the inside chamber bottom using thermally conductive tape.

## REFERENCES

1. Endres, K. J.; Hill, J. A.; Lu, K.; Foster, M. D.; Wesdemiotis, C., Surface Layer Matrix-Assisted Laser Desorption Ionization Mass Spectrometry Imaging: A Surface Imaging Technique for the Molecular-Level Analysis of Synthetic Material Surfaces. *Analytical Chemistry* **2018**, *90* (22), 13427-13433.
2. Hill, J. A. Surface Layer Matrix-Assisted Laser Desorption Ionization Time of Flight Mass Spectrometry (SL-MALDI-TOF MS) Analysis of Polymer Blend Surface Composition. University of Akron, 2017.
3. Lu, K. Optimization of Sublimation Conditions for Surface Layer Matrix-assisted Laser Desorption Ionization Time of Flight Mass Spectrometry Imaging (SL-MALDI- ToF MSI) of Polymer Surfaces. University of Akron, 2018.
4. Guo, H. Improving Matrix Deposition for Surface Layer Matrix-Assisted Laser Desorption/Ionization Time-of-Flight Mass Spectrometry Imaging. University of Akron, 2019.
5. Myers, D., *Surfaces, interfaces, and colloids : principles and applications*. 2nd ed. ed.; Wiley-VCH: 1999.
6. Wu, D. T.; Fredrickson, G. H., Effect of Architecture in the Surface Segregation of Polymer Blends. *Macromolecules* **1996**, *29* (24), 7919-7930.
7. Wang, S.-F.; Li, X.; Agapov, R. L.; Wesdemiotis, C.; Foster, M. D., Probing Surface Concentration of Cyclic/Linear Blend Films Using Surface Layer MALDI-TOF Mass Spectrometry. *ACS Macro Letters* **2012**, *1* (8), 1024-1027.
8. Wang, S.-F. Synthesis and Characterization of Surface Relaxations of Macrocyclic Polystyrenes and Interfacial Segregation in Blends with Linear Polystyrenes. University of Akron, 2011.
9. Watson, J. T.; Sparkman, O. D., *Introduction to mass spectrometry: instrumentation, applications and strategies for data interpretation*. 4th ed.; John

Wiley & Sons: 2007.

10. Li, L., *MALDI Mass Spectrometry for Synthetic Polymer Analysis: Mass Spectrometry for Synthetic Polymer Analysis*. John Wiley & Sons: Hoboken, United States, 2009.

11. Räder, H.; Schrepp, W., MALDI-TOF mass spectrometry in the analysis of synthetic polymer. *Acta Polymerica* **1998**, 49 (6), 272-293.

12. Hoffmann, E. d.; Stroobant, V., *Mass spectrometry: principles and applications*. 3rd ed.; J. Wiley: 2007.

13. Bahr, U.; Deppe, A.; Karas, M.; Hillenkamp, F.; Giessmann, U., Mass spectrometry of synthetic polymers by UV-matrix-assisted laser desorption/ionization. *Analytical Chemistry* **1992**, 64 (22), 2866-2869.

14. Fouquet, T.; Mertz, G.; Desbenoit, N.; Frache, G.; Ruch, D., TOF-SIMS/MALDI-TOF combination for the molecular weight depth profiling of polymeric bilayer. *Materials Letters* **2014**, 128, 23-26.

15. Hill, J. A.; Endres, K. J.; Mahmoudi, P.; Matsen, M. W.; Wesdemiotis, C.; Foster, M. D., Detection of Surface Enrichment Driven by Molecular Weight Disparity in Virtually Monodisperse Polymers. *ACS Macro Letters* **2018**, 7 (4), 487-492.

16. Hill, J. A.; Endres, K. J.; Meyerhofer, J.; He, Q.; Wesdemiotis, C.; Foster, M. D., Subtle End Group Functionalization of Polymer Chains Drives Surface Depletion of Entire Polymer Chains. *ACS Macro Letters* **2018**, 7 (7), 795-800.

17. Endres, K. J. *Mass Spectrometry Methods For Macromolecules: Polymer Architectures, Cross-Linking, and Surface Imaging*. University of Akron, 2019.

18. Weidner, S. M.; Falkenhagen, J., Imaging mass spectrometry for examining localization of polymeric composition in matrix-assisted laser desorption/ionization samples. *Rapid Communications in Mass Spectrometry* **2009**, 23 (5), 653-660.

19. Hanton, S. D.; Parees, D. M., Extending the solvent-free MALDI sample preparation method. *Journal of the American Society for Mass Spectrometry* **2005**, *16* (1), 90-93.
20. Trimpin, S.; Deinzer, M. L., Solvent-Free MALDI-MS for the Analysis of a Membrane Protein via the Mini Ball Mill Approach: Case Study of Bacteriorhodopsin. *Analytical Chemistry* **2007**, *79* (1), 71-78.
21. Fernández, R.; Garate, J.; Martín-Saiz, L.; Galetich, I.; Fernández, J. A., Matrix Sublimation Device for MALDI Mass Spectrometry Imaging. *Analytical Chemistry* **2019**, *91* (1), 803-807.
22. Zhang, Z. Effect Of Chain End Functional And Chain Architecture On Surface Segregation. University of Akron, 2017.
23. Huizing, L. R. S.; Ellis, S. R.; Beulen, B. W. A. M. M.; Barré, F. P. Y.; Kwant, P. B.; Vreeken, R. J.; Heeren, R. M. A., Development and evaluation of matrix application techniques for high throughput mass spectrometry imaging of tissues in the clinic. *Clinical Mass Spectrometry* **2019**, *12*, 7-15.